IEEE Access
Multidisciplinary ⋮ Rapid Review ⋮ Open Access Journal

Received June 8, 2021, accepted June 22, 2021, date of publication June 29, 2021, date of current version July 21, 2021.

Digital Object Identifier 10.1109/ACCESS.2021.3093277

A Compressive Receding Horizon Approach for Smart Home Energy Management

JOAQUIM LEITÃO[1], CARLOS M. FONSECA[1], PAULO GIL[1,2], BERNARDETE RIBEIRO[1], (Senior Member, IEEE), AND ALBERTO CARDOSO[1]

[1]Department of Informatics Engineering, Center for Informatics and Systems of the University of Coimbra (CISUC), 3030-790 Coimbra, Portugal
[2]Centre of Technology and Systems (CTS), Department of Electrical and Computer Engineering, NOVA School of Science and Technology, Universidade NOVA de Lisboa at Caparica (UNINOVA), 2829-516 Caparica, Portugal

Corresponding author: Joaquim Leitão (jpleitao@dei.uc.pt)

This work was supported by the National Funds through the Foundation for Science and Technology (FCT), Instituto Público (I.P.), within the scope of the projects Center for Informatics and Systems of the University of Coimbra (CISUC) under Grant UID/CEC/00326/2020 and Centre of Technology and Systems (CTS) under Grant UID/EEA/00066/2019. The work of Joaquim Leitão was supported in part by the Portuguese Funding Institution FCT, in part by the Human Capital Operational Program (POCH), and in part by the European Union (EU) through the Ph.D. Grant under Grant SFRH/BD/122103/2016.

ABSTRACT Current increases in the demand for electricity require sustainable energy management measures and have promoted the adoption of clean and renewable sources, particularly at the residential building level. Active demand management is usually carried out through load shifting based on specific techniques, such as optimisation, heuristics, model-based predictive control and machine learning methodologies. This work addresses the problem of residential load scheduling via optimisation techniques. A compressive receding horizon strategy is proposed for week-ahead load shifting, and the selection is driven by traditional receding horizon and day-ahead allocation strategy misalignment, with weekly household appliance usage patterns. The proposed approach is compared with receding horizon and day-ahead scheduling techniques over 30 different weeks for a prototypical smart home with non-controllable demand, which is representative of a four-resident family and includes micro power generation and battery storage. The simulation results confirm the validity of the proposed strategy in the context of household appliance scheduling problems and show competitive electricity costs and resident discomfort performance compared to state-of-the-art approaches. Furthermore, the proposed compressive receding horizon strategy fully exploits weather and photovoltaic generation forecasts to promote self-consumption and grid demand stress reduction while providing environmental gains and financial benefits to the utility service and consumers, particularly in the case of simultaneously scheduling a huge number of households.

INDEX TERMS Home energy and water management systems, mixed-integer programming, optimal scheduling, receding horizon, smart homes.

NOMENCLATURE

Parameter Scalars

α	Household electricity bill weight
λ_d	Average toilet flush rate at day time
λ_e	Average toilet flush rate in the evening
λ_n	Average toilet flush rate at night
τ_t	Need to schedule a tumble dryer load in the current horizon
τ_w	Need to schedule a washing load in the current horizon
SOC_0	Battery state of charge at horizon start
SOC_{max}	Maximum battery state of charge
SOC_{min}	Minimum battery state of charge
C	Household contracted power
C_b	Battery storage capacity
d_0	First day of the horizon
d_d	Minimum delay between consecutive dishwasher loads
d_f	Last day of the horizon
d_w^{first}	Number of days from the start of the horizon without washer or dryer loads
h	Number of slots in any given day
l_d	Number of slots of a full dishwasher load
l_t	Number of slots for a full tumble dryer load

The associate editor coordinating the review of this manuscript and approving it for publication was Behnam Mohammadi-Ivatloo.

l_w Number of slots for a full washing load
n_c Battery charge efficiency
n_d Battery discharge efficiency
o_t Number of slots from the start of the horizon assigned to the tumble dryer machine
o_w Number of slots from the start of the horizon assigned to the washing machine
p^{bc}_{max} Maximum battery charge power
p^{bd}_{max} Maximum battery discharge power
p^{bc}_{min} Minimum battery charge power
p^{bd}_{min} Minimum battery discharge power
p^{full}_{d} Average power of the dishwasher
p^{full}_{p} Maximum power of the pump system
p^{full}_{t} Average power of the tumble dryer when the entire slot is used
p^{last}_{t} Average power of the tumble dryer in the last operating slot
p^{full}_{w} Average power of the washing machine when the entire slot is used
p^{last}_{w} Average power of the washing machine in the last slot
q_{max} Maximum water flow of the pump system
q_{min} Minimum water flow of the pump system
q_f Average water volume per toilet flush
q^{full}_{w} Average nonpotable water flow of the washing machine when the entire slot is used
q^{last}_{w} Average nonpotable water flow of the washing machine in the last slot
S Grid power injection incentives
s^{first}_{d} Number of slots on the first day of the horizon without dishwasher loads
T Number of slots in the scheduling horizon
V_0 Water volume stored in the tank at the start of the horizon
V_{max} Maximum water tank storage
V_{min} Minimum water tank storage

Parameter Vectors

$\boldsymbol{\zeta}^d$ Household resident preference for dishwasher operation
$\boldsymbol{\zeta}^t$ Household resident preference for tumble dryer operation
$\boldsymbol{\zeta}^w$ Household resident preference for washing operation
$\mathbf{B}$ TOU utility grid tariffs
$\mathbf{E^{home}}$ Non-controllable household electricity demand
$\mathbf{F}$ Non-controllable household toilet flush events
$\boldsymbol{PV}$ Photovoltaic electricity generation

Decision Variable Vectors

$\mathbf{b^c}$ Battery system charging flag
$\mathbf{d}$ Dishwasher operation
$\mathbf{e}^+$ Positive household electricity balance
$\mathbf{e}^-$ Negative household electricity balance
$\mathbf{e}$ Household electricity balance
$\mathbf{p^{bc}}$ Battery system charging power
$\mathbf{p^{bd}}$ Battery system discharging power
$\mathbf{q}$ Pump system operation
$\mathbf{r^{bc}b^c}$ Battery charging ratio and charging flag product
$\mathbf{r^{bc}}$ Battery system charging ratio
$\mathbf{r^{bd}b^c}$ Battery discharging ratio and charging flag product
$\mathbf{r^{bd}}$ Battery system discharging ratio
$\mathbf{sd}$ Dishwasher operation start
$\mathbf{SOC}$ Battery system state of charge
$\mathbf{st}$ Tumble dryer operation start
$\mathbf{sw}$ Clothes washing operation start
$\mathbf{t}$ Tumble dryer operation
$\mathbf{V}$ Tank water volume
$\mathbf{w}$ Clothes washing operation

I. INTRODUCTION

Electrical energy is a key resource for humans that powers important infrastructures and services. In recent decades, sustained worldwide increases in demand have been observed, which have contributed to a global energy crisis [1]. To address the current energy challenges, utility companies have been tasked with increasing the generation output and power grid transmission and distribution capacity. Recently, the ''smart'' grid paradigm has attracted interest from both academia and industry. A smart grid promises to be fully automated, efficient, intelligent and reliable. This new-generation infrastructure is supported by the bidirectional flow of information and power between customers and utility. Demand-side load coordination is promoted, which provides benefits to both utility services through improved peak demand prediction and response and customers through bill minimisation via load management. Within demand-side entities, considerable attention has been devoted to residential buildings because they represent a significant worldwide electricity demand share [2].

In summary, building energy efficiency is enabled via consumption reduction or load shifting policies [3]. Consumption reduction proposes to curtail demand by upgrading to energy-efficient devices and disconnecting unnecessary loads, whereas load shifting is regulated by efficient, less intrusive, and cost-effective consumption shifting policies. The popularity of load shifting in residential buildings is, to some extent, linked to the less expensive and less intrusive intervention mechanisms [4].

Demand-side management (DSM) and demand response (DR) programs are highlighted in the literature for load shifting [5]. In DSM, energy efficiency and bill reduction techniques, namely, building design and construction improvements, customer awareness and incentive tariffs, are commonly considered [6]. Conversely, DR focuses on real-time grid price adjustments and incentive payments, in which demand-side load changes are promoted to reduce demand at specific periods [7]. In [8], the problem of

scheduling household electrical loads was defined as an instance of a demand responsive appliance (DRA) optimal scheduling problem. In DRA problems, the operation of electrical appliances is deferred to periods of cheaper electricity or higher generation to improve certain parameters, such as electricity consumption, electricity cost, peak-to-average ratio (PAR) or resident comfort. As noted in [8], the DRA optimal scheduling problem is often framed as a multidimensional constrained nonlinear problem. In recent literature surveys and publications [3], [8], common approaches employed within DSM and DR programs are categorised into the following four groups: (i) mathematical optimisation, (ii) heuristic-based, (iii) model-based predictive control, and (iv) machine learning approaches.

In mathematical optimisation-based allocation, load scheduling is carried out by solving an optimisation problem. Electricity bills and resident discomfort are the two most prevalent criteria [9], and a number of constraints restrict resident comfort and controllable appliance operations. Within mathematical optimisation-based allocation, linear programming (LP) problems, in which a linear objective function and constraints are specified, are highlighted [3]. For LP problems, mixed-integer linear programming (MILP) variants, where integer and noninteger decision variables are considered, have received particular attention for home energy management. Because both integer and noninteger decision variables are specified in MILP problems, these variables are particularly suited for describing domestic appliance operations. While proper discrete operation modelling, i.e., appliances requiring only to be turned on or off is allowed by integer decision variables, appliances whose operation is continuous in time are modelled by noninteger decision variables. Concerning the scheduling horizon, day-ahead (DA) controllable appliance scheduling is usually favoured among mathematical optimisation-based strategies [10]–[14]. For modelling electricity demand from non-controllable appliances, in some works, this contribution is completely neglected [10], [11], while in other works, it is explicitly accounted for [12]–[16]. Within non-controllable demand modelling, stochastic and robust programming are emphasised in explicit uncertainty modelling [17]. In stochastic programming, uncertainties are modelled via random variables, with the expected objective function value being optimised. Scenario-based instances are often considered, and they rely on concrete uncertainty realisations to approximate the aforementioned expected function values. Moreover, interval-based uncertainty modelling is adopted in robust programming, and this method considers realisations with worse problem solution impacts.

Heuristics and metaheuristics are commonly preferred over mathematical optimisation when exact solutions cannot be computed within a feasible timeframe. These approaches rely on high-level sampling procedures and sacrifice accuracy, precision and optimality in favour of speed. DA allocation remains the norm, with genetic algorithms [18], [19] and swarm intelligence-based techniques representing common choices. Particle swarm optimization is the most popular swarm-based heuristic [5], [20]–[22], and other include artificial bee colonies [23], polar bears [8], grey wolf optimization [24] and differential evolution [25]. Explicit multiobjective optimisation problem instances have also been addressed by evolutionary approaches; see, e.g., [26]. They compute Pareto frontier solutions that cannot be improved according to any criterion without decreasing performance with respect to other criteria.

In model-based predictive control (MPC), appliance scheduling is formulated as a receding horizon (RH) optimal control problem. It consists of implementing an iterative process, observing the system state at each discrete time instant, and computing a horizon-dependent optimal control sequence. Only the first control action is implemented, and the procedure is repeated in the next discrete time step. MPC smart home appliance scheduling is mainly concerned with thermostatically regulated loads, such as heating, ventilation and air-conditioning (HVAC) units [27]–[29] and refrigerators [30]. Nonetheless, it has also been recently applied for load coordination of multiple customer microgrids [31], [32].

Finally, intelligent approaches to identifying optimal appliance operation times have been the subject of growing attention from the scientific community and practitioners in recent years. Much of this recent attention has been focused on the widespread use of smart grid digital sensor technologies [33]. In a recent literature survey [33], intelligent approaches to improving home energy efficiency were categorised into (i) nature-inspired, (ii) machine learning (ML), and (iii) multi-agent systems. The reader is directed to [33] and references therein for a more detailed overview of the application of intelligent approaches for home energy management and efficiency.

Nature-inspired techniques take the form of the above discussed heuristics and metaheuristics. ML techniques are subsequently categorized into (ii-a) supervised learning, (ii-b) unsupervised learning and (ii-c) reinforcement learning (RL). The main difference between supervised and unsupervised learning techniques is that the former relies on a set of labelled input-output pairs while the latter does not. Supervised learning techniques exploited the aforementioned labelled data to learn a function that maps inputs to desired outputs. Within the scope of home energy management, supervised learning techniques have been primarily considered to forecast electricity demand [34], generation [35] or grid prices [36]. Within supervised learning techniques, artificial neural networks (ANNs) are highlighted for their performance and popularity when forecasting data of different natures, and they have already been successfully applied for pattern recognition and clustering [37]. In recent years, the adoption of ANNs has been growing in popularity, mostly due to the advent of deep learning (DL). The application of DL techniques has achieved promising results that have even surpassed human performance for certain types of

problems [33]. However, unsupervised learning techniques aim to find patterns in unlabelled data. Their main advantage over supervised learning alternatives is concerned with the fact that they do not require labelled data, which can be expensive to obtain. As pointed out in [33], clustering, dimensionality reduction and matrix completion represent the most common strategies in this category for application to home energy management. RL [38] comprehends intelligent agents and iteratively learns how to perform a given task in a surrounding environment. At each iteration, the current environmental state is observed, an action is chosen and performed, and a reward is received based on the resulting environmental impact. Q-learning is one of the most popular RL algorithms and has been considered in collaborative and noncollaborative scenarios [39], [40]. The main Q-learning limitation concerns the state and action space discretisation, thus limiting smaller resolution scalability. Deep RL (DRL) algorithms address this limitation via deep learning-based nonlinear action-value function estimation with infinite action space. In [41], smart home appliance scheduling was carried out by hierarchical DRL, while the peak-to-average load ratio was minimized in [42] based on a distributed DRL framework. Finally, among techniques involving multiagent systems, game theory-based approaches are highlighted [3], [33]. In multiagent frameworks, each agent must find a strategy that improves its utility function while also taking into consideration the global objectives and objectives of other agents. Cooperative and noncooperative games represent the two main categories of game theory approaches, and they are distinguished based on cooperation or the lack of cooperation between individual agents [3]. In [33], the adoption of cooperative game theory was highlighted for DR, particularly in the presence of binding agreements. As an example, in [43], DSM is achieved in a smart microgrid system via a game-theoretic strategy in which individual agents collaborate together to minimise service costs and electricity bills.

Two main findings emerge from the literature on household appliance scheduling. First, non-controllable electricity demand is not considered in some works, e.g., [10], [26], [31], which can have a potentially negative infrastructure impact, particularly if carried out at a large scale. This effect results from a finite supply power, which, if surpassed, may damage existing infrastructure and cause power outages. Stochastic programming-based and robust non-controllable demand modelling, as suggested in [12], [15], [25], prevents these situations and guarantees a minimum probability of meeting supply bounds. Second, DA scheduling is favoured over longer scheduling horizons, namely, one week. While daily household dishwashers, HVACs or lighting operations are required, clothing washer and dryer operations are less frequent, e.g., on a weekly basis. Under DA scheduling, washer or dryer allocation on any day of the week is optional. The only exception concerns the last day provided no previous scheduling has been set. Taking into account the electricity bill criterion, these loads are likely delayed until the last day, which may not be the most profitable choice. The adoption of longer, e.g., weekly, horizons within RH frameworks addresses this problem by considering operation on different days before a decision is made. Concerning weekly RH strategies, as the horizon start is progressively shifted throughout the week, a portion of the next week is covered. Similar problems to DA allocation are found in this framework in terms of optional appliance scheduling over the incomplete following week.

This work addresses the problem of week-ahead household appliance scheduling for DSM electrical energy efficiency. The main contribution of this work is the proposal of a novel mathematical optimisation-based compressive receding horizon (CRH) approach, which is proposed to address the aforementioned issues of RH-, MPC- and DA-based week-ahead appliance scheduling. Similarly, standard RH schemes are allocated for each new day of the week. Only the first day of planned operation is implemented. Unlike traditional RH, successively smaller horizons are considered, and they shift the first day and fix the last day. CRH assessment against RH and DA strategies is carried out based on a prototypical smart home scenario. Scheduling of four electrical appliances, namely, clothing washer, tumble dryer, dishwasher and electrical pump, is studied. Micropower generation is also available through photovoltaic (PV) panels and a battery for power storage. Controllable and non-controllable demand is modelled by real-world historical data, while micro PV generation is described by panel models and weather forecast data. The contributions of this work are summarized as follows:

- This work proposes a new CRH optimisation-based approach for week-ahead home controllable appliance scheduling. Controllable appliance operation is rescheduled every new day of the week under updated representative non-controllable demand and local power generation profiles. Daily rescheduling is performed to address model degradation and accommodate unexpected events, such as additional controllable load operation outside of typical usage.
- The proposed CRH optimisation-based scheduling approach is compared against state-of-the-art DA and traditional RH strategies according to weekly electricity costs and resident discomfort criteria.
- The CRH optimisation-based scheduling approach is also compared against both the ideal allocation and typical appliance operation.

The remainder of this document is organized as follows. The prototypical smart home environment is described in Section II. A formal definition of optimisation problems instantiated in the proposed CRH approach is provided in Section III, and the proposed approach is detailed in Section IV. CRH, RH and DA appliance allocation is discussed in Section V, and the obtained domestically controllable appliance operation schedules are compared against those referred to as ideal allocation and typical

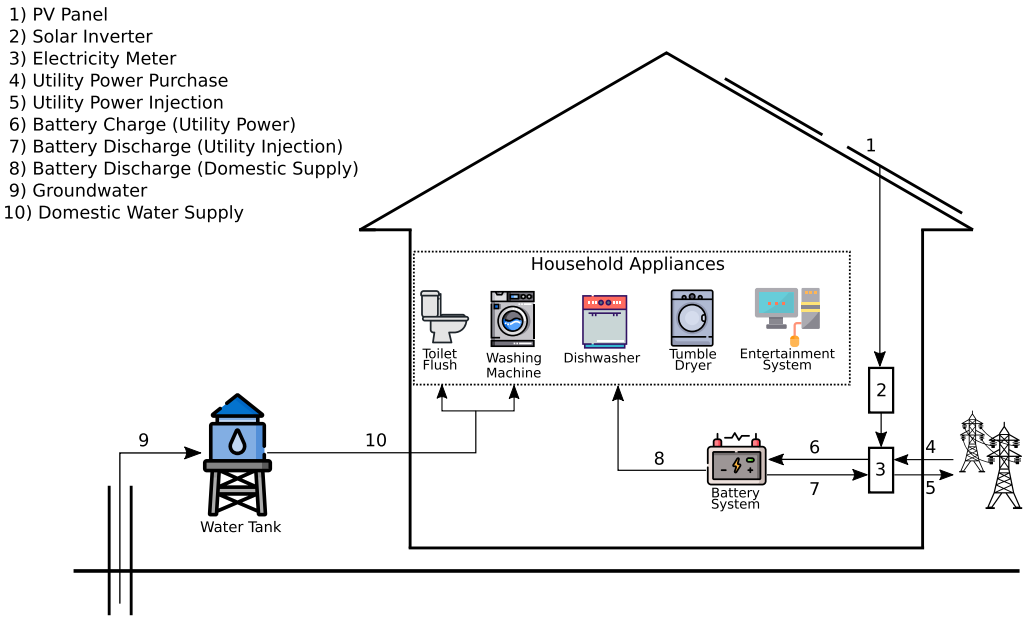

FIGURE 1. Problem scenario.[1]

appliance operation. Finally, the concluding remarks are provided in Section VI.

II. HOUSEHOLD CHARACTERISATION

A prototypical single-family smart home is presented in Figure 1, and it consists of household electrical appliances, external water tanks, battery storage, and PV panels. PV panels are used for micro power generation, whereas excess electrical energy is stored in a battery for later domestic supply or grid injection. The external water tank is included for nonpotable groundwater storage and used for domestic supply. The existing tank structure is supplied with groundwater by an electrical pump system. Although groundwater lacks proper treatment and is therefore not suited for consumption, showering or dishwashing, it can be used for toilet flushing and clothes washing, which promotes potable water savings [44].

Local electrical appliances can be powered by multiple sources, including PV micro generation, battery power or public grids. Micro PV generation can be used directly for supplying demand, charging battery systems or performing public grid injection. In the case of grid power injection, financial compensation proportional to the injected power is obtained. The battery system can be charged based on local micro PV generation or relying on public grid purchases. Stored battery power can be subsequently used for either domestic supply or public grid reinjection.

A smart home is assumed to be equipped with a home energy management system (HEMS) for monitoring domestic demand and managing certain electrical appliances, namely, clothes washer, tumble dryer, dishwasher and electrical pump system. The HEMS is also responsible for micro PV generation self-consumption coordination, grid power injection, battery system charging and discharging. The washing machine is a *Candy* GSV128T3S operated on the Mix program, with a duration of 105 minutes, consumption of 0.98 kWh and consumption of 57 litres. The tumble dryer machine is a *Bosch* WTG85230EE operated on the *Cotton* program, with a duration of 203 minutes and consumption of 6.08 kWh. The dishwasher machine is a *Bosch* SMS25AW05E operated on the *Normal* program, with a duration of 120 minutes and total consumption of 1.3 kWh. The battery storage system is modelled as in [45], considering a single lead-acid battery with a 2.4 kWh capacity. Finally, the electrical pump is characterized by a 30 l/h maximum flow rate and 1 kW peak power, while the external water tank has a maximum capacity of 334 l. In the current smart home case study, daily dishwasher loads are considered, while a single weekly washer and tumble dryer load is intended to be performed. For the operation of the electrical pump system and management of the battery system, their respective operation is determined based on the current nonpotable water volume stored in the tank and the battery SOC value.

Electricity and nonpotable water demand resulting from household appliances not managed by the HEMS are treated as non-controllable loads and modelled to represent a possible real-world scenario for a four-resident household. Non-controllable electricity demand is described based on real-world historical aggregated records available in Pecan Street's Dataport dataset,[2] which was collected over a two-year period on an hourly basis for a single-family home. Concerning nonpotable water demand, only two sources are

[1] Icons taken from https://www.flaticon.com.

[2] https://dataport.cloud

TABLE 1. Toilet flush Poisson distribution parameters.

Parameter	Value	Description
λ_d	0.75 flush/h	Day rate (8h-16h)
λ_e	1.25 flush/h	Evening rate (16h-0h)
λ_n	0.5 flush/h	Night rate (0h-8h)
q_f	6 litre/flush	Total volume per flush

considered, namely, toilet flushing and washing machine operations. The nonpotable water demand of the washing machine is modelled based on the selected program water consumption. However, toilet flushing is modelled as in [20], [23] through a Poisson distribution parametrised by the Alliance for Water Efficiency[3] (Table 1).

The Poisson distribution describes independent random discrete events with known average time in between them but unknown exact timing. The Poisson probability distribution expresses the probability of observing a given number of events in a time period. Let X be a discrete random Poisson variable with probability density $f_X(k)$, which is given by (1) [46].

$$f_X(k) = P(X = k) = \frac{\lambda^k e^{-\lambda}}{k!} \tag{1}$$

where e denotes the exponential function and λ refers to the average number of events, which parameterises the X distribution: $X \sim Po(\lambda)$, with $\mathbb{E}(X) = \lambda$ being the expected value of random variable X.

Micropower generation is forecasted based on the PV panel model and parametrisation in [47], global forecast system cloud coverage data collected via the *PVLIB Python* library [48] v0.6.0, solar radiation model *parametrization model C* [49] and deterministic cloud radiation attenuation model [50]. PV panel radiation is estimated over an inclined plane for a cloudless atmosphere over a 10 m^2 PV area with a 35 degree inclination towards the equator. Battery system storage is modelled through the so-called *state of charge* (SOC), which is defined as the ratio of the current battery capacity to nominal capacity [45]. Utility grid purchases are billed according to a time of use (TOU) tariff, which considers a publicly available rate structure from a utility company. In this work, electricity is billed at 0.2029 c.u./kWh (currency unit per kilowatt-hour) between 7 am and 11 pm and billed at 0.0969 c.u./kWh from 0 am to 7 am and from 11 pm to 0 am.

Furthermore, household resident discomfort observed as a result of HEMS washer, tumble dryer and dishwasher scheduling solutions is considered. Following [26], resident discomfort is defined for a given controllable appliance as the negative impact on resident lifestyle resulting from appliance operations deviating from the typical usage carried out by household residents. Resident discomfort is evaluated separately for each appliance, i.e., clothes washer, tumble dryer and dishwasher. Following [26], resident discomfort is computed as the percentage of operations of the corresponding appliance, which is not performed by residents, in each time period of interest. For the electrical pump, no specific discomfort model is included since there is no interaction between residents and the water pump.

[3]http://www.allianceforwaterefficiency.org

III. OPTIMISATION PROBLEM FORMULATION

Controllable load scheduling is performed by solving an MILP problem instance over a given horizon while considering representative non-controllable electricity and water demand profiles and micro power generation forecasts. All MILP instances share the same set of parameters, variables, objective functions and constraints, and they differ solely based on certain parameter values. A time domain discretisation is performed, and the scheduling horizon is split into T hourly slots numbered from 1 to T, with the i^{th} slot covering the period from hour $i-1$ to hour i. In the remainder of this section, vectors are distinguished from scalars, with the former shown in bold.

A. PARAMETERS

The first (d_0) and last $\left(d_f\right)$ days of the horizon are defined for each problem instance, with $d_f = 7$ denoting the last day of the week and $d_0 = 1, \ldots, d_f$. In addition, the number of slots $h = 24$ in each day and the corresponding length of each scheduling horizon $T = \left(d_f - d_0 + 1\right) \cdot h$ are defined for each problem instance. The duration of a washing machine load is defined in parameter $l_w = 2$ and expressed in the number of time slots. Parameters $l_t = 4$ and $l_d = 2$, which are also expressed in the number of slots, define tumble dryer and dishwasher load durations, respectively.

Washer, tumble dryer and dishwasher electricity and nonpotable water demand (when required) are considered constant throughout their respective programs. As a complete dishwasher load takes exactly two slots, a constant average power per slot parameter $p_d^{full} = 0.65$ kW is defined. The aforementioned average power of the dishwasher is determined by dividing the full program power of this appliance, which is specified in Section II for a *Bosch* SMS25AW05E dishwasher, for the respective duration, which is expressed in the number of time slots. Concerning the washer and tumble dryer machines, as the duration of their respective operation cycles is not a multiple of the slot length, their operation only partially occupies the last operating slot. Consider, e.g. the clothes washing machine. In any given washer load, the appliance is turned on during the entire first operating slot, and the first 45 minutes of its second operating slot. From minute 46 to 60 of its second slot, this appliance is turned off. As such, demand from the clothes washing and tumble dryer machines is smaller during their last operating slot. Parameter $p_w^{\text{full}} = 0.56$ kW models the average washing machine power when the entire slot is used, while parameter $p_w^{last} = 0.42$ kW models the average washing machine power in the last slot. Parameter $p_t^{full} = 1.8$ kW models the average tumble dryer power when the entire slot is used, and parameter $p_t^{last} = 0.68$ kW models the average tumble dryer power in the last slot. Concerning the washer and dryer machines, their respective power when

the entire slot is used is determined by dividing the full program power by its duration, which is expressed in the number of time slots. According to the program duration and consumption specified in Section II, for the *Candy* GSV128T3S washing machine, an average power of $p_w^{\text{full}} = \frac{e_w^{cycle}}{l_w - 1} = 0.56$ kW is obtained when the entire slot is used, with $e_w^{cycle} = 0.98$ kWh denoting the total demand of the complete clothes washing operation cycle. Concerning the tumble dryer machine, an average power of $p_t^{full} = \frac{e_t^{cycle}}{l_t - 1} = 1.8$ kW is obtained for the *Bosch* WTG85230EE tumble dryer, with $e_t^{cycle} = 6.08$ kWh denoting the total demand of the tumble dryer operation cycle. For the two machines, the electricity demand during the last slot is computed by subtracting the total demand in previous slots from the total demand of the corresponding program. Finally, the average power for each machine in the last slot is computed by dividing the demand in that slot by the length of each slot. In the case of the washing machine, $p_w^{last} = \frac{e_w^{cycle} - (l_w - 1) \cdot p_w^{\text{full}}}{\Delta t} = 0.42$ kW, with $e_w^{cycle} = 0.98$ kWh as defined above, and $\Delta t = 1$ h represents the length of each slot. For the tumble dryer, $p_t^{last} = \frac{e_t^{cycle} - (l_t - 1) \cdot p_t^{full}}{\Delta t} = 0.68$ kW, with $e_t^{cycle} = 6.08$ kWh as defined above, and $\Delta t = 1$ h represents the length of each slot.

A similar modelling of the nonpotable water flow of the washing machine is carried out based on its program duration and total consumption, as presented in Section II. As such, parameter $q_w^{full} = \frac{w_w^{cycle}}{l_w - 1} = 32.57$ l/h models the washing machine average nonpotable water flow when the entire slot is used, with $w_w^{cycle} = 57$ l denoting the total nonpotable water demand of a complete washing machine cycle. Finally, parameter $q_w^{last} = \frac{w_w^{cycle} - (l_w - 1) \cdot q_w^{full}}{\Delta t} = 24.43$ l/h models the washing average nonpotable water flow in the last slot, with $w_w^{cycle} = 57$ l as defined above, and $\Delta t = 1$ h represents the length of each slot. Concerning the pump system, parameters $q_{min} = 0$ l/h and $q_{max} = 30$ l/h define the minimum and maximum pump system groundwater flow rates, respectively. Parameter $p_p^{\text{full}} = 1$ kW models the pump system power at maximum flow. At any given slot, the pump system power is modelled as a fraction of full operation power p_p^{full}.

Binary parameter $\tau_w \in \{0, 1\}$ describes the need to wash and dry a load of clothes in the current scheduling horizon, with $\tau_w = 1$ if it is true and $\tau_w = 0$ otherwise. The binary parameter $\tau_t \in \{0, 1\}$ is defined for the tumble dryer machine with a similar purpose. Therefore, $\tau_t = 1$ if a tumble dryer load must be scheduled in the current horizon, and $\tau_t = 0$ otherwise. The washing machine is assumed to have precedence over the dryer, such that a new dryer load starts in the slot immediately after the last washer slot. Parameters $o_w \in \{0, \ldots, l_w - 1\}$ and $o_t \in \{0, \ldots, l_t - 1\}$ are defined to ensure the continuity of washing and dryer operations at the start of each new horizon. Parameter o_w specifies the number of slots assigned to the washing machine starting from the new horizon. In addition, parameter o_t specifies the number of slots assigned to the dryer starting from the new horizon. On the first optimisation problem instance, it is assumed that $o_w = o_t = 0$ because overnight washer or dryer loads are not considered at the beginning of any new given week.

For any given MILP problem instance, scheduling a given washer and dryer load is only permitted from a given day onwards, e.g., the first day or any other day. This restriction ensures minimum consecutive washer or dryer operation delays. Parameter $d_w^{first} \in \{0, \ldots, d_f - 1\}$ specifies the number of days without washer or dryer loads starting from the new horizon. Overall, consecutive washer or dryer loads must be scheduled with a minimum three-day delay. For the dishwasher, a minimum delay of $d_d = 11$ time slots is imposed for consecutive loads. Parameter $s_d^{\text{first}} \in \{0, \ldots, h - l_d\}$ imposes a dishwasher delay in the first day of new MILP problem instances, thus specifying the number of slots in the first day of the horizon without dishwasher loads. In the first optimization problem instance, no delay is imposed among washer, dryer and dishwasher loads, resulting in $d_w^{first} = s_d^{\text{first}} = 0$.

Parameters $V_{max} = 334$ l and $V_{min} = 100$ l define the water tank volume boundaries. Parameter V_0 defines the tank volume at the start of the current horizon, with $V_0 = V_{min}$ in the first optimisation problem instance. Parameter vector $\mathbf{F}$ of length T specifies representative non-controllable household toilet flush events over the horizon. Concerning toilet flush events, the average nonpotable water volume per toilet flush is represented by the parameter $q_f = 6$ l/flush. Each vector element F_i, which is expressed in flush/h and with $i = 1, \ldots, T$, represents non-controllable household toilet flush events estimated to occur at the start of slot i of the horizon. Each element F_i (with $i = 1, \ldots, T$) is modelled based on appropriate Poisson distributions, whose parametrization is presented in Table 1. As noted in Section II, the aforementioned parametrisation of the Poisson probability distributions is provided by the Alliance for Water Efficiency.[4]

Concerning non-controllable household electricity demand, it is represented by vector $\mathbf{E^{home}}$, which is also of length T. Each vector element E_i^{home} (expressed in kW and with $i = 1, \ldots, T$) represents the estimated non-controllable household electricity demand at the start of slot i of the horizon. Each element E_i^{home} (with $i = 1, \ldots, T$) is modelled based on real-world historical aggregated electricity demand records collected from Pecan Street's Dataport dataset[5] for a single-family home and the same period as the scheduling horizon of the respective optimisation problem instance. Local PV panel generation is represented by parameter vector $\boldsymbol{PV}$ of length T. Each vector element PV_i (expressed in kW and with $i = 1, \ldots, T$) represents the estimated micro PV generation at the start of slot i of the horizon. Each element PV_i (with $i = 1, \ldots, T$) is modelled based on PV generation forecasts computed for the slot in question. As mentioned

[4] http://www.allianceforwaterefficiency.org
[5] https://dataport.cloud

in Section II, micro PV generation is forecasted for each slot based on the PV panel model and parametrization in [47], and solar radiation estimates are also performed for the respective slot of the current week. Micro PV generation is forecasted considering a 10 m^2 PV area with a 35 degree inclination towards the equator. As stated in Section II, solar radiation estimates are computed based on the solar radiation model *Parametrization Model C* [49], which considers the attenuation effects of clouds in Earth's atmosphere via cloud coverage data collected from the Global Forecast System using the *PVLIB Python* library [48] v0.6.0 and the deterministic cloud radiation attenuation model [50].

The reader should note that within the scope of this work, the abovementioned parameter vector elements F_i and E_i^{home} (with $i = 1, \ldots, T$) do not consider actual historical readings. Instead, for each slot of the horizon, a representative demand profile is derived for each source through a process described in detail in Section V.

Parameter $C = 5.75$ kVA denotes the contracted power suggested for a typical family of four, and it imposes a threshold on the total demand at each horizon slot. Parameter vector **B**, length T, represents the TOU utility grid tariffs. Elements B_i and $i = 1, \ldots, T$ represent TOU tariffs at the start of slot i of the horizon and are expressed in c.u./kWh. $B_i = 0.0969$ c.u./kWh for $i \; mod \; h \leq e_{pr}^{start} \vee i \; mod \; h > e_{pr}^{end}$, where $e_{pr}^{start} = 8$, $e_{pr}^{end} = 22$, $i \; mod \; h$ denotes the remainder of the integer division of i by h and c.u. denotes the currency units. Moreover, $B_i = 0.2029$ c.u./kWh for $e_{pr}^{start} < i \; mod \; h \leq e_{pr}^{end}$. Concerning the local micro generation surplus grid injection, a constant income for power grid injection is defined in parameter $S = 0.05$ c.u./kWh.

Parameters $SOC_{min} = 0.3$ and $SOC_{max} = 0.9$ define the admissible battery system SOC, while SOC_0 models battery system SOC at the start of each given horizon. As previously stated, within the scope of the current work, the battery system SOC is defined as the ratio of current battery capacity to nominal capacity [45]. Moreover, in the first optimisation problem instance, battery system SOC at the start of the horizon is defined to take its minimum value, i.e., . $SOC_0 = SOC_{min}$ in the first optimisation problem instance. Battery system modelling and parametrisation follows that presented in [45], which includes the battery system capacity, charging and discharging efficiencies, and charging and discharging power bounds. Thus, based on the above cited work, parameter $C_b = 2.4$ kWh represents the battery system capacity, with parameters $n_c = 0.85$ and $n_d = 0.95$ describing the battery system charging and discharging efficiency, respectively. The minimum and maximum battery system charging power values are specified by parameters $p_{min}^{bc} = 0$ kW and $p_{max}^{bc} = 0.48$ kW, respectively. Similarly, the minimum and maximum battery system discharging power values are specified by parameters $p_{min}^{bd} = 0$ kW and $p_{max}^{bd} = 0.48$ kW, respectively.

Household resident discomfort with planned washer, dryer and dishwasher operations is modelled separately for each appliance and following [26]. As stated in Section II, resident discomfort is computed as the percentage of operations of the corresponding appliance that is not performed by residents in each slot of the horizon. To compute the resident discomfort associated with the planned operation of a given appliance, a parameter vector describing resident preference for the operation of each appliance in question in each slot of the horizon is specified. As such, parameter vectors $\boldsymbol{\zeta}^w$, $\boldsymbol{\zeta}^t$ and $\boldsymbol{\zeta}^d$, which are all of length h, are defined to describe resident preference for the operation of the washer, dryer and dishwasher in each slot of the horizon. As such, each element ζ_i^{w} (with $i = 1, \ldots, h$) denotes the residents' preference for the operation of the washing machine in slot i of the horizon. Similarly, elements ζ_i^{t} and ζ_i^{d} (with $i = 1, \ldots, h$) are defined similarly for the dryer and dishwasher for each slot i of the horizon. Following [26], each element ζ_i^{w}, ζ_i^{t} and ζ_i^{d} (with $i = 1, \ldots, h$) is computed as the percentage of operations of the corresponding appliance performed by residents in slot i of the horizon. As such, each element ζ_i^{w}, ζ_i^{t} and ζ_i^{d} (with $i = 1, \ldots, h$) is represented by a real number in the [0,1] range. A value closer to 1 suggests higher washer, dryer or dishwasher operation preferences during slot i of the horizon and 0 otherwise. The reader is directed to Sections III-C and [26] for a more detailed explanation of resident discomfort modelling. Finally, parameter α weights the household electricity bill contribution to the MILP problem instance objective function.

B. DECISION VARIABLES

A total of $11\,T$ decision variables are defined for each optimisation problem instance solved on each day of the week, where T is the horizon length parameter:

1) Binary variable vectors **w**, **t** and **d** describe the washer, dryer and dishwasher operations, respectively. Elements $w_i, t_i, d_i \in \{0, 1\}, i = 1, \ldots, T$ take the value 1 if the corresponding appliance is operating at time slot i and 0 otherwise.
2) Vector **q**, of length T, where $q_i \in \mathbb{R}_0^+$ and $i = 1, \ldots, T$ represent the electrical pump system water flow rate at each horizon slot.
3) Binary variable vectors **sw**, **st**, **sd** of length T describe the slot of the horizon in which a new washer, tumble dryer or dishwasher load is started, respectively. Elements $sw_i, st_i, sd_i \in \{0, 1\}$ (with $i = 1, \ldots, T$) take the value 1 if a new corresponding load starts at slot i of the horizon and 0 otherwise.
4) Vector **V** of length T, where $V_i \in \mathbb{R}_0^+$, $i = 1, \ldots, T$ models the tank water volume at the end of slot i.
5) Vector **SOC** of length T (with SOC_i, $i = 1, \ldots, T$), which describes the battery system SOC value at each slot end.
6) Vector **e**, of length T, where $e_i \in \mathbb{R}$, $i = 1, \ldots, T$ represents the domestic electricity balance, which is defined as the difference between demand and generation in slot i of the horizon.

7) Vectors $\mathbf{e}^+, \mathbf{e}^-$ of length T, where $e_i^+, e_i^- \in \mathbb{R}_0^+$, $i = 1, \ldots, T$ model positive and negative electricity balance.
8) Vectors $\mathbf{p^{bc}}$ and $\mathbf{p^{bd}}$ of length T, whose elements p_i^{bc} and p_i^{bd}, $i = 1, \ldots, T$, which describe battery charging and discharging power at each horizon slot, respectively.
9) Binary vector $\mathbf{b^c}$ of length T, where b_i^c, $i = 1, \ldots, T$ take the value 1 if the battery system is being charged at horizon slot i, and 0 otherwise.
10) Vectors $\mathbf{r^{bc}}$ and $\mathbf{r^{bd}}$ of length T, with r_i^{bc}, r_i^{bd} and $i = 1, \ldots, T$ representing the battery system charging and discharging ratio at each horizon slot, respectively.
11) Auxiliary vectors $\mathbf{r^{bc}b^c}$ and $\mathbf{r^{bd}b^c}$ of length T, where $r^{bc}b_i^c$, $r^{bd}b_i^c$, $i = 1, \ldots, T$, model the problem variable products $r_i^{bc} \cdot b_i^c$ and $r_i^{bd} \cdot b_i^c$ at each horizon slot, respectively.

C. CRITERIA

The appliance scheduling problem aims to minimise two conflicting criteria involving the electricity bill (EB) and resident discomfort (RD), which are defined according to (2).

$$\begin{aligned} EB &= \Delta t \sum_{i=1}^{T} \left(B_i e_i^+ - S e_i^- \right) \\ RD &= 1 - \frac{RD_w + RD_t + RD_d}{d_f - d_0 + 1} \end{aligned} \tag{2}$$

where $\Delta t = 1$ h, $RD_w = \varrho_w \sum_{d_g=d_0}^{d_f} \sum_{i=1}^{h} \zeta_i^{\mathrm{w}} w_{(d_g-d_0)h+i}$, $RD_t = \varrho_t \sum_{d_g=d_0}^{d_f} \sum_{i=1}^{h} \zeta_i^{\mathrm{t}} t_{(d_g-d_0)h+i}$, and, finally, the term $RD_d = \varrho_d \sum_{d_g=d_0}^{d_f} \sum_{i=1}^{h} \zeta_i^{\mathrm{d}} d_{(d_g-d_0)h+i}$ is defined as in [26].

The EB criterion presented in (2) was originally defined as the sum of a piecewise function over each slot of the horizon. According to this function, each term of the sum defines the EB for the slot in question. For each slot i of the horizon (with $i = 1, \ldots, T$), if the corresponding electricity balance is positive or null, i.e., $e_i \geq 0$, then the EB for that slot is given by multiplying the respective electricity balance value by the respective TOU grid tariff, which is given by B_i, for $i = 1, \ldots, T$. However, if the electricity balance at slot i of the horizon (with $i = 1, \ldots, T$) is negative, i.e., $e_i < 0$, then the EB for that slot is given by multiplying the respective electricity balance value by the constant income for power grid injection (defined by parameter S). In (2), a linear expression is presented for the EB criterion, and it is derived by splitting the domestic electricity balance at each slot of the horizon into positive and negative values, i.e., e_i^+ and e_i^-, for $i = 1, \ldots, T$.

Concerning the RD criterion, the term RD_w, which is defined in (2), represents the weighted sum over the entire horizon of the resident washing machine preference in the slots during which this appliance is operating. This sum is weighted by ϱ_w. Indeed, it is noted that $w_{(d_g-d_0)\,h+i}$ denotes the washing machine operational state at slot i of day d_g, with $d_g = d_0, \ldots, d_f$ and $i = 1, \ldots, h$. For any $d_g = d_0, \ldots, d_f$ and $i = 1, \ldots, h$, $w_{(d_g-d_0)h+i} \in \{0, 1\}$, the product $\zeta_i^{\mathrm{w}} w_{(d_g-d_0)h+i}$ either outputs ζ_i or 0. As such, $\sum_{d_g=d_0}^{d_f} \sum_{i=1}^{h} \zeta_i^{\mathrm{w}} w_{(d_g-d_0)h+i}$ gives the sum of the resident washing machine preference in the slots during which this appliance is turned on. The terms RD_t and RD_d are defined for the dryer and dishwasher with similar meanings, respectively, and they are weighted by ϱ_t and ϱ_d, respectively. Within the scope of the current work, equal-valued priority weights are considered, with $\varrho_w = \varrho_t = \varrho_d = \frac{1}{3}$.

EB and RD criteria are combined in a single objective function by means of a weighted sum, thus leading to a single-objective problem instance. Criterion normalization is further carried out to obtain an objective function insensitive to individual criterion scaling. The reader is referred to the supplemental material in Appendices A and B for a detailed presentation of the criteria normalization process. The RD criterion is already restricted to the [0, 1] interval, whereas the normalised EB is defined in (3).

$$EB^* = \frac{\sum_{i=1}^{T} \left(B_i e_i^+ - S e_i^- \right) - EB_{min}}{EB_{max} - EB_{min}} \tag{3}$$

where $EB_{min} = S \sum_{i=1}^{T} \left(\omega + E_i^{home} - PV_i \right)$ is the electricity bill lower bound, $EB_{max} = \sum_{i=1}^{T} B_i \left(\Omega + E_i^{home} - PV_i \right)$ is the corresponding upper bound, and $\omega = \frac{q_{min}}{q_{max}} p_p^{full} + p_{min}^{bc} - p_{max}^{bd}$ and $\Omega = p_d^{full} + p_p^{full} + p_w^{full} + p_t^{full} + p_{max}^{bc} - p_{min}^{bd}$.

D. OBJECTIVE

The appliance scheduling problem concerns the minimisation of the weighted sum of the electricity bill and resident discomfort criteria, and it is defined in (4).

$$\min \alpha EB^* + (1 - \alpha)\, RD \tag{4}$$

subject to (5)–(22):

1)
$$e_i^+ \geq 0 \quad e_i^- \geq 0 \quad e_i^+ - e_i^- = e_i \tag{5}$$
for $i = 1, \ldots, T$. As (4) is minimised and $B_i > S$ for any slot, solutions with only one nonzero value of e_i^+ or e_i^- for each slot $i = 1, \ldots, T$ are favoured. Moreover, it follows from constraint $e_i^+ - e_i^- = e_i$ that the nonzero value of e_i^+ or e_i^- corresponds to the electricity balance in slot i, $i = 1, \ldots, T$.
2) The electricity balance is computed in (6) as the difference between electricity demand and local generation while accounting for a smaller washer and dryer demand in their last operating slots.
$$\begin{aligned} e_i = {} & d_i p_d^{full} + \frac{q_i}{q_{max}} p_p^{full} + E_i^{home} - PV_i \\ & + wi\, p_w^{full} + sw_{(i-l_w+1)} \left(p_w^{last} - p_w^{full} \right) \\ & + t_i p_t^{full} + st_{(i-l_t+1)} \left(p_t^{last} - p_t^{full} \right) \\ & + p_i^{bc} - p_i^{bd} \quad i = 1, \ldots, T \end{aligned} \tag{6}$$

considering $sw_j = st_j = 0$ for $j \leq 0$. Washing machine electricity demand at slot $i = 1, \ldots, T$ is given by $w_i p_w^{full} + sw_{(i-l_w+1)} \left(p_w^{last} - p_w^{full}\right)$. If slot i is the last washing machine operation slot, then $w_i = 1$ and $sw_{(i-l_w+1)} = 1$ because this load started at slot $i - l_w + 1$. In this case, washing machine electricity demand at horizon slot i becomes $p_w^{full} + p_w^{last} - p_w^{full} = p_w^{last}$. However, if slot i is not the last washing machine operating slot, then $sw_{(i-l_w+1)} = 0$ and washing machine electricity demand at horizon slot i becomes $w_i p_w^{full}$. A similar rationale can be applied for dryer machine electricity demand.

3) Decision variables $w_i, t_i, d_i, sw_i, st_i, sd_i, i = 1, \ldots, T$ are restricted to binary values. Elements of each appliance operation status vector, namely, w_i, t_i, d_i, $i = 1, \ldots, T$, are also correlated with the corresponding appliance operation start vectors **sw**, **st** and **sd**, respectively. Moreover, vector elements q_i and $i = 1, \ldots, T$ are restricted to take real values between q_{min} and q_{max}:

$$\begin{aligned} & w_i,\ t_i,\ d_i \in \{0,1\} \quad q_{min} \leq q_i \leq q_{max} \\ & sw_i,\ st_i,\ sd_i \in \{0,1\} \quad d_i = \sum_{\substack{j=i-l_d+1 \\ j\geq 1}}^{i} sd_j \\ & \tau_w\, w_i = \tau_w \sum_{\substack{j=i-l_w+1 \\ j\geq 1}}^{i} sw_j \quad \tau_t\, t_i = \tau_t \sum_{\substack{j=i-l_t+1 \\ j\geq 1}}^{i} st_j \\ & \qquad\qquad i = 1, \ldots, T \end{aligned} \tag{7}$$

For any given slot i, $i = 1, \ldots, T$, the washing machine can be in operation or turned off. If turned on, then the operation started at slot $j \in [i - l_w + 1, i]$, with $i - l_w + 1 \geq 1$ to ensure that the starting slot remained within the predefined horizon. In this case, $\sum_{\substack{j=i-l_w+1 \\ j\geq 1}}^{i} sw_j = 1$; otherwise, $\sum_{\substack{j=i-l_w+1 \\ j\geq 1}}^{i} sw_j = 0$. Similar constraints are defined for the dryer and dishwasher.

4) Controllable and noncontrollable electricity demand is required to remain below the contracted power C at any slot i, $i = 1, \ldots, T$:

$$E_i^{home} + w_i\, p_w^{full} + t_i\, p_t^{full} + d_i\, p_d^{full} + \frac{q_i}{q_{max}}\, p_p^{full} \leq C \tag{8}$$

5) The washing machine load precedence over the tumble dryer is specified in (9). A new tumble dryer load is defined to start in the slot that immediately follows the end of a washing load. Moreover, either one or no washing and tumble dryer loads are scheduled in the current horizon. The constraint in (9) is defined only in problem instances for which washing and tumble dryer load scheduling are required. This constraint is turned on or off according to parameter τ_w.

$$\tau_w \left(l_w + \sum_{j=1}^{T} sw_j \cdot j \right) = \tau_w \sum_{j=1}^{T} st_j \cdot j \tag{9}$$

Considering that a single washer and dryer load is scheduled at most, $\sum_{j=1}^{T} sw_j \cdot j$ indicates the horizon slot of a new washing load start. Similarly, $\sum_{j=1}^{T} st_j \cdot j$ provides the horizon slot of a new dryer load start. As such, if $\tau_w = 1$ and $sw_i = 1$, $\sum_{j=1}^{T} st_j \cdot j = l_w + i$, for a given horizon slot i. This compels the subsequent tumble dryer load to start immediately after the corresponding washing machine operation is completed.

6) Clothes washing and tumble dryer scheduling in the current horizon is ensured in (10), according to parameters τ_w and τ_t. As $\tau_w, \tau_t \in \{0,1\}$, a single or no washer and dryer load can be scheduled in the current horizon. The start of a new washer or dryer load is further conditioned by the corresponding program length. Moreover, overnight washer and dryer load continuity were also ensured.

$$\begin{aligned} & \sum_{i=1}^{T-l_w-l_t+1} sw_i = \tau_w \qquad \sum_{i=T-l_w-l_t+2}^{T} sw_i = 0 \\ & \sum_{i=1}^{T-l_t+1} st_i = \tau_t \qquad \sum_{i=T-l_t+2}^{T} st_i = 0 \\ & \sum_{i=1}^{o_w} w_i = o_w \qquad \sum_{i=1}^{o_w} t_i = 0 \\ & \sum_{i=o_w+1}^{o_w+o_t} t_i = o_t \end{aligned} \tag{10}$$

With $\sum_{i=1}^{T-l_w-l_t+1} sw_i = \tau_w$ and $\sum_{i=T-l_w-l_t+2}^{T} sw_i = 0$, a new washing machine load cannot start in the last $l_w + l_t - 1$ slots of the horizon, which is imposed to ensure that the load finishes during the assigned horizon. Similarly, tumble dryer loads cannot start in the last $l_t - 1$ slots of the horizon. Finally, constraint $\sum_{i=1}^{o_w} w_i = o_w$ forces overnight washing load allocation during the first o_w slots of the horizon. A similar constraint is defined for the tumble dryer. When overnight washing machine allocation is considered, i.e., $o_w > 0$, constraint $\sum_{i=1}^{o_w} t_i = 0$ ensures that the dryer remains turned off during overnight operation of the washing machine.

7) Clothes washing load delay in consecutive weeks is imposed by (11) to prevent new washing machine load starts in the first d_w^{first} days of the horizon:

$$\sum_{i=1}^{d_w^{\text{first}}\, h} sw_i = 0 \tag{11}$$

8) The dishwasher is scheduled every day of the horizon. Daily dishwasher load scheduling is imposed in (12).

$$\sum_{j=1}^{h-l_d+1} sd_{g+j} = 1 \qquad \sum_{j=h-l_d+2}^{h} sd_{g+j} = 0 \tag{12}$$

where $g = (d_g - d_0)\,h$ and $d_g = d_0, \ldots, d_f$.

9) Dishwasher loads need to be scheduled in accordance with the delay specified by parameter d_d. In (13), at least d_d slots are required to separate new dishwasher loads.

$$\sum_{j=1}^{\min(d_d-1;T-i)} sd_{i+j} \leq (1 - sd_i) \tag{13}$$

for $i = 1, \ldots, T$. Dishwasher load delays are extended to the first slots of the horizon in (14) to account for dishwasher loads prior to the start of the horizon, i.e., overnight dishwasher operation. As such, a new dishwasher load can never be scheduled in the first s_d^{first} slots of the first day:

$$\sum_{i=1}^{s_d^{first}} sd_i = 0 \tag{14}$$

10) The water tank volume is bounded in (15) by parameters V_{min} and V_{max}.

$$V_{min} \leq V_i \leq V_{max} \tag{15}$$

where $i = 1, \ldots, T$. Following [51], the volume of water stored in the tank at the end of each slot of the horizon is modelled in (16). As such, the tank water volume storage is computed as the difference between the pump flow and domestic demand, which considers smaller clothes washing nonpotable water demand in the last washer operating slot.

$$V_i = V_0 + \Delta t \sum_{j=1}^{i} \left(q_j - F_j q_f - w_j q_w^{full}\right) - \Delta t \sum_{\substack{j=l_w \\ i \geq l_w}}^{i} sw_{j-l_w+1} \left(q_w^{last} - q_w^{full}\right) \tag{16}$$

where $i = 1, \ldots, T$ and $\Delta t = 1$ h denotes the slot length.

11) The battery system SOC is modelled at each slot end according to (17). Following [45], SOC is modelled by the difference between battery system charging and discharging, which considers charging and discharging efficiencies.

$$SOC_i = SOC_{i-1} + n_c \cdot r_i^{bc} b^c + \frac{r_i^{bd} b^c - r_i^{bd}}{n_d} \qquad i = 1, \ldots, T \tag{17}$$

where SOC_0 is a parameter corresponding to the battery system SOC at the horizon start. The SOC upper and lower bounds are defined in (18) for each slot i of the horizon (with $i = 1, \ldots, T$).

$$SOC_{min} \leq SOC_i \leq SOC_{max} \quad , i = 1, \ldots, T \tag{18}$$

The battery charging and discharging ratios are evaluated in (19) as the ratio between battery charging or discharging power at slot i of the horizon ($i = 1, \ldots, T$), and battery system capacity C_b.

$$\begin{aligned} r_i^{bc} &= \frac{p^{bc}}{C_b} \quad r_i^{bc} \leq b_i^c \\ r_i^{bd} &= \frac{p^{bd}}{C_b} \quad r_i^{bd} \leq \left(1 - b_i^c\right) \quad i = 1, \ldots, T \end{aligned} \tag{19}$$

Battery charging and discharging are delimited in (20) according to parameters p_{min}^{bc}, p_{max}^{bc}, p_{min}^{bd} and p_{max}^{bd}.

$$p_{min}^{bc} \leq p_i^{bc} \leq p_{max}^{bc} \quad p_{min}^{bd} \leq p_i^{bd} \leq p_{max}^{bd}, \qquad i = 1, \ldots, T \tag{20}$$

Finally, variable products $r_i^{bc} \cdot b_i^c$, $i = 1, \ldots, T$ are modelled in (21) by auxiliary variables $r^{bc}b_i^c$, which are defined for each slot i of the horizon ($i = 1, \ldots, T$).

$$\begin{aligned} r^{bc}b_i^c &\leq \frac{p_{max}^{bc}}{C_b} b_i^c \\ r^{bc}b_i^c &\leq r_i^{bc} \\ r^{bc}b_i^c &\geq r_i^{bc} - \left(1 - b_i^c\right) \frac{p_{max}^{bc}}{C_b} \\ r^{bc}b_i^c &\geq 0 \quad i = 1, \ldots, T \end{aligned} \tag{21}$$

In the above products, $r_i^{bc} \cdot b_i^c$, r_i^{bc} represent continuous variables, b_i^c are binary variables, with $i = 1, \ldots, T$. Continuous variables r_i^{bc} and $i = 1, \ldots, T$ are bounded by $0 \leq r_i^{bc} \leq \frac{p_{max}^{bc}}{C_b}$ for $i = 1, \ldots, T$. As such, if r_i^{bc} takes its upper bound, then $r^{bc}b_i^c = \frac{p_{max}^{bc}}{C_b} b_i^c$, $i = 1, \ldots, T$, and an upper bound on auxiliary variables $r^{bc}b_i^c$, $i = 1, \ldots, T$, is defined. Moreover, if $b^c = 0$, a lower bound on $r_i^{bc}b^c$ is already imposed, i.e., $r^{bc}b_i^c \geq 0$, $i = 1, \ldots, T$. However, if $b^c = 1$, then $r^{bc}b_i^c = r_i^{bc}$, which motivates the upper bound constraint $r^{bc}b_i^c \leq r_i^{bc}$. In addition, if $b^c = 1$, then the third inequality states that $r_i^{bc}b^c \geq r_i^{bc}$, which in conjunction with the second inequality ensures that $r_i^{bc}b^c = r_i^{bc}$, as desired. Otherwise, if $b^c = 0$, then the third inequality states that $r_i^{bc}b^c$ must be greater than a negative number. Finally, the last inequality states that $r^{bc}b_i^c$ has to be greater than or equal to 0, which is desired because both r_i^{bc} and b^c are lower bounded by 0. Auxiliary variable vector elements $r^{bd}b_i^c$, $i = 1, \ldots, T$ are modelled in (22) in a similar way, thus describing the problem

variable products $r_i^{bd} \cdot b_i^c$ for each slot i of the horizon (with $i = 1, \ldots, T$):

$$\begin{aligned} r^{bd} b_i^c &\leq \frac{p_{max}^{bd}}{C_b} b_i^c \\ r^{bd} b_i^c &\leq r_i^{bd} \\ r^{bd} b_i^c &\geq r_i^{bd} - \left(1 - b_i^c\right) \frac{p_{max}^{bd}}{C_b} \\ r^{bd} b_i^c &\geq 0 \quad i = 1, \ldots, T \end{aligned} \tag{22}$$

Finally, it should be mentioned that in (4), both the normalized weekly electricity bill (EB^*) and RD are unitless and defined in the interval [0,1]. Moreover, as $0 \leq \alpha \leq 1$, the expression in (4) is also constrained to the interval [0,1]. As stated, the relative importance of weekly electricity bill minimisation is represented by parameter α. This parameter describes the electricity bill contribution to the objective function of the MILP problem instantiated at each new day of the horizon. When smaller α weight values are considered, resident discomfort minimisation is assigned higher preference. Conversely, stronger importance to weekly electricity bill minimisation is assigned by higher α weights.

IV. COMPRESSIVE RECEDING HORIZON-BASED SMART HOME APPLIANCE SCHEDULING

As emphasised in [3], washer and dryer machines are two examples of common HEMS managed appliances. Washer and dryer loads are generally operated a few times a week in typical households. The washer and dryer operation frequencies are dependent on many factors, including the family size and lifestyle. In this context, optimal load planning requires choosing the day of the week and the slot of the day for which the chosen criteria are optimised. While optional allocation of loads that are not needed every day can be considered in DA frameworks, the choice of operating a load on a specific day does not consider subsequent days. Given the popularity of electricity bill and peak load criteria, such optional load scheduling is likely to be discarded for the sake of criteria improvement.

This work addresses the limitations of DA smart home load shifting by proposing week-ahead appliance operation planning under a CRH-based approach. Similarly, RH appliances are initially scheduled over a one-week horizon from Monday to Sunday. Appliance operation times are determined by solving an MILP problem instance as described in Section III. Representative non-controllable electricity and nonpotable water demand profiles are considered over a weekly horizon. Micro PV generation forecasts are also retrieved over the same weekly horizon. The first day of the planned operation was implemented, and the procedure was repeated at the start of the next day. A six-day horizon is now considered, and it was obtained by shifting the first day and maintaining the last day of the horizon unchanged, i.e., from Tuesday to Sunday. The new MILP problem instance is solved considering recalculated non-controllable (electricity and nonpotable water) demand profiles along with updated PV generation forecasts. The procedure was sequentially repeated until the end of the corresponding week. The proposed CRH-based appliance scheduling strategy is outlined in Algorithm 1 and sketched in Figure 2.

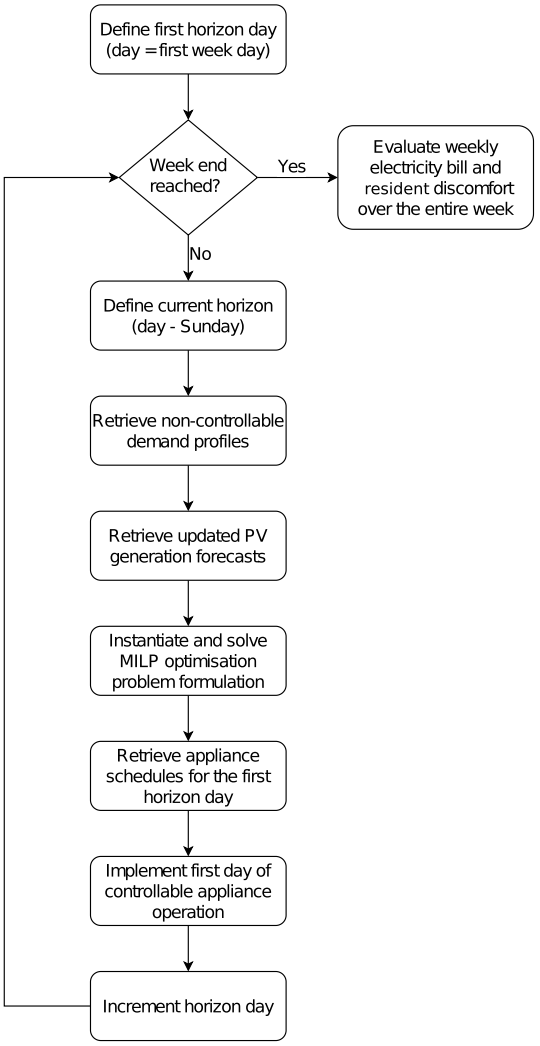

FIGURE 2. CRH-based scheduling strategy flow chart.

Algorithm 1 Compressive Receding Horizon

for each day of the week **do**

a. Define the optimisation problem instance horizon (day – Sunday)
b. Retrieve non-controllable electricity and nonpotable water profiles from historical records
c. Retrieve updated micro PV generation forecasts
d. Instantiate MILP problem formulation
e. Solve MILP instance (min (4) s.t. (5)–(22))
f. Retrieve scheduling solution for the first horizon day
g. Implement the first day of controllable appliance operation

end for

Differences between the CRH-based strategy proposed in this work, which are presented in Algorithm 1 and Figure 2, and DA appliance scheduling must be clearly noted. As discussed in the previous paragraph, in CRH-based scheduling, controllable loads are initially scheduled over a complete week. At the start of each new day of the week, controllable load rescheduling is promoted, and it covers a period from the current day of the week to the last day of the week. As stated above, motivations for daily rescheduling stem from exponential weather forecasts; consequently, micro PV generation forecasts and errors with longer horizons are considered. However, although controllable appliance allocation is performed for DA scheduling for each day of the week, it is only ever planned over a one-day horizon. As previously stated, the fact that only a single day is considered lead to the optional allocation of loads that are not used on a daily basis, such as the washer and dryer, for each day of the week. To the best of the authors' knowledge, the novel CRH-based framework represents the first time that a CRH into week-ahead household appliance scheduling has been proposed. Moreover, the inclusion of both noncontrollable demand profiles and micro power generation forecasts improves the controllable appliance schedule robustness, which has not been extensively considered in the literature.

By considering a fixed-width horizon, from the second day onwards, the traditional RH covers the current week and part of the next week. As controllable loads are scheduled over the entire horizon, drawbacks similar to those discussed for DA scheduling are found for loads not operated every day. Their allocation during part of the next week is optional, and considering common criteria, they will likely be discarded. By planning appliance operation over a given week and relying on progressively smaller scheduling horizons, typical weekly usage trends of some appliances can be properly addressed. This compressive rescheduling can address PV generation forecast errors stemming from unreliable weather forecasts by adjusting the controllable load operation. In addition, other unexpected events requiring load scheduling adjustment, namely, extra dishwasher, clothes washer or tumble dryer loads, can also be accommodated. Moreover, extensions to the proposed CRH strategy can also be considered, such as by generalising the daily appliance rescheduling to any slot of the horizon. In this way, unexpected events, such as imposing additional operation constraints and load scheduling needs, can be properly accommodated.

It should be mentioned at this point that CRH deployment on an HEMS demands real-time, reliable and robust data along with state estimation to ensure constraint feasibility, which implies continuous monitoring of the household environment, particularly the tank volume bounds and contracted power. Although real-world deployments are beyond the scope of the current paper, the reader is referred to [52]–[54] and references therein for a thorough discussion on these issues.

V. APPLIANCE SCHEDULING RESULTS

The proposed CRH approach is employed in week-ahead appliance scheduling based on the minimisation of the weighted sum of weekly electricity bills and resident discomfort. Controllable load allocation is carried out over 30 different weeks (from March 2018 to February 2019) for the smart home environment described in Section II. CRH-based appliance operation schedules and the corresponding criteria evaluation are compared against DA, standard RH, ideal allocation, and considering a typical user operation. The popularity of DA and RH motivated the selection of these two particular strategies, which provide benchmarks for assessing the proposed CRH scheme. For ideal allocation, a lower bound on the scheduling performance is imposed. Ideal scheduling makes use of a priori knowledge of future non-controllable demand and micro PV generation. A typical allocation mimics the residents' behaviour with respect to appliance operation based on historical records.

In the case of DA scheduling, a single-day horizon MILP problem is formulated and solved by considering micro PV generation forecasts and non-controllable electricity and nonpotable water profiles. The solution is then implemented on the prescribed day. For the standard RH, load planning is carried out for each new day of the week over a 7-day horizon. Only the first day of planned appliance operation is implemented. Micro PV generation forecasts and non-controllable electricity and nonpotable water profiles cover a 7-day period. Concerning the ideal allocation, a single MILP instance is solved for each week based on the real-world historical non-controllable demand and PV generation. Finally, in the case of the typical appliance allocation modus operandi, appliance operation data are directly retrieved from historical records. Thus, no MILP optimisation problem instance is solved.

For each week, a non-controllable electricity demand profile is determined by taking the 85^{th} percentile of one-year historical records in the period of 10 weeks before and after the week in question. As an example, for the week starting on 18/02/2019, historical records from 11/12/2017 to 30/04/2018 are considered. Historical electricity demand records are used to compute the aforementioned representative demand profile, and they are collected from Pecan Street's Dataport dataset[6] for a single-family home and the period of interest. Regarding non-controllable nonpotable water demand, the aforementioned probabilistic Poisson distribution-based modelling of this non-controllable demand source is exploited. As such, the underlying representative profile is computed for each slot of each week by multiplying the 85^{th} percentile of the Poisson distribution assigned to that slot by the average volume per toilet flush. The Poisson distribution parameters and average volume per toilet flush are presented in Table 1. Concerning micro PV generation, its output is forecasted for each slot of the horizon for a 10 m^2 PV area with a 35 degree inclination

[6]https://dataport.cloud

towards the equator. Micro PV generation forecasts are computed based on the aforementioned PV panel model and parametrization in [47], solar radiation estimates determined using the solar radiation model *Parametrization Model C* [49], cloud coverage data collected from the Global Forecast System via the *PVLIB Python* library [48] v0.6.0, and a deterministic model, which is used express the attenuation effects of cloud in Earth's atmosphere over solar radiation [50]. Finally, washer, dryer and dishwasher preferences, which were originally formulated in [26], are derived from one-year historical records. As such, for each element of parameter vectors $\boldsymbol{\zeta}^w$, $\boldsymbol{\zeta}^t$ and $\boldsymbol{\zeta}^d$, specified in (2), the percentage of operations of the corresponding appliance performed by residents in each slot of the horizon is only computed based on the aforementioned one-year period. As an example, for the week starting on 18/02/2019, historical appliance usage records from 18/02/2018 to 17/02/2019 are considered.

Regarding typical appliance allocation, for each of the 30 weeks, washer, dryer and dishwasher operations are retrieved from the respective historical household demand records and the typical electrical pump system operation is defined as follows. When the volume of water drops below 10% available storage, i.e., when $V_i \leq V_{min} + 0.1\,(V_{max} - V_{min})$, with $i = 1, \ldots, T$ denoting the current slot of the horizon and V_i the water tank volume at slot i, the underlying pump is turned on until the tank is full, i.e., $V_i = V_{max}$. During the tank refill, the pump is set to run at full power as long as contracted power is not exceeded. For typical battery storage management, a similar strategy is followed. When the battery capacity drops below 10% of the available SOC, i.e., when $SOC_i \leq SOC_{min} + 0.1\,(SOC_{max} - SOC_{min})$, with $i = 1, \ldots, T$ denoting the current slot of the horizon and SOC_i denoting the battery SOC at slot i, the battery is charged until its capacity is full, i.e., $\mathrm{SOC}_i = SOC_{max}$. During battery charging, maximum possible charging power is deployed as long as contracted power is not surpassed at each horizon slot. During battery system charging, available local micro power generation is favoured over grid purchases. Moreover, once the battery is fully charged, its available power is favoured for domestic supply.

For each of the 30 weeks, appliance scheduling under CRH, RH, DA and ideal allocation is carried out for 5 different household electricity bill weight values: (i) strict resident discomfort minimisation ($\alpha = 0$); (ii) strict electricity bill minimisation ($\alpha = 1$); (iii) equal criteria importance ($\alpha = 0.5$); (iv) higher resident discomfort minimisation without completely disregarding electricity bill ($\alpha = 0.25$); and (v) higher electricity bill minimisation without completely disregarding resident discomfort ($\alpha = 0.75$). Finally, it should be mentioned that all optimisation problem instances are solved using the SCIP solver v6.0.0 [55], [56] running on an Ubuntu 16.04 machine with 504 GB RAM and a dual 2.2 GHz Intel Xeon Silver 4214 CPU with a 16.5 MB cache.

A. COMPRESSIVE RECEDING HORIZON

The proposed CRH approach is employed in scheduling controllable appliances for the 30 weeks considered. In each week, controllable load planning is carried out for the aforementioned five electricity bill weight values, for which non-controllable demand profiles and micro PV generation forecasts are determined.

In the case of $\alpha = 0$, the washer, dryer and dishwasher operations are scheduled for higher resident preference periods. Across 30 weeks, washer and dryer loads are always scheduled for the same slots of the day, which coincide with on-peak tariffs. However, for different weeks, they are operated on different days of the horizon. The washing machine is operated within slots 16 and 17, i.e., from 3 pm to 5 pm, whereas the tumble dryer is operated from slot 18 to 21, i.e., from 5 pm to 9 pm. Regarding the dishwasher, nighttime operations that coincide with off-peak tariffs are preferred. This load is mainly scheduled from 2 am to 4 am, i.e., from slots 3 to 4, albeit its start is anticipated by one slot in a few weeks. Concerning the water pump, its operation does not influence the resident discomfort criterion. As such, it is only scheduled to ensure water tank volume requirements and to match the contracted power constraint based on non-controllable electricity and nonpotable water demand profiles. Intense and prolonged pump system operation immediately before high non-controllable nonpotable water demand is commonly observed. Considering that these periods coincide with on-peak tariffs, the aforementioned pump system operation contributes to a weekly electricity bill increase.

For $\alpha = \{0.25; 0.5\}$, washer, dryer and dishwasher scheduling follows the same pattern reported for $\alpha = 0$. For $\alpha = 0.75$, washer and dryer loads are no longer strictly performed during on-peak billing periods. Instead, for some weeks, they are shifted to nighttime hours from 0 am to 6 am. Moreover, off-peak dishwasher allocation is maintained, thus optimising both criteria. Pump system operation is shown to vary the most with increasing α weights. As electricity bill minimisation becomes more important, i.e., higher α weights are considered and extended and intense on-peak electrical pump activity is replaced with smaller flow rate and off-peak allocation. As a result of the shorter pump operation and a smaller flow rate, a reduction in pump electricity demand and thus a lower weekly electricity bill is observed. For larger α weights, i.e., $\alpha = 0.75$, smoother pump operation is responsible for the water volume storage decrease over the entire week, remaining closer to minimum capacity.

Finally, for $\alpha = 1$, resident discomfort is excluded and appliance allocation is carried out solely under electricity bill minimisation. For this situation, a more extreme off-peak allocation is observed. Washer and dryer machine operations are entirely shifted to off-peak billing periods. On some days of some weeks, washer and dryer machine operations spanned over two separate days, which occurs when a new washer load is deployed at slots 22 or 23 of a given day of

the week. As a result of the aforementioned washer and dryer off-peak shifting, dishwasher and electrical pump system operation need to be adjusted accordingly. Concerning the dishwasher, its operation is allocated to different slots of each day of the week than those reported for smaller α weights but remained constrained to off-peak billing periods. In addition, electric pump system operation is coordinated with (i) other controllable appliances and (ii) nonpotable water demand to minimise weekly electricity bills while ensuring feasible schedules. Smaller pump flow rates are also observed and mostly allocated to off-peak slots, except when the specified minimum tank volume cannot be ensured by any other means. In this case, the electrical pump system is scheduled to on-peak billing slots. Finally, for each week, lower pump flow rates are reported on the last day of the scheduling horizon. The aforementioned smaller pump flow rates stem from the minimisation of the weekly electricity bill considered for this α weight. The consequences of smaller pump flow rates are twofold: first, lower water tank volume storage is reported on the last day of each week; and second, a smaller pump system electricity demand is registered on the last day of each week, thus contributing to weekly electricity bill reduction.

A controllable appliance operation determined for each α weight is subsequently simulated over each week, and it considers the actual non-controllable demand and micro generation. In all simulated weeks, tank overflow is observed for some slots, which takes place when the stored volume calculated according to (16) exceeds the maximum capacity. This phenomenon is due to non-controllable nonpotable water demand overestimation in the representative profile. To maintain robust appliance schedules with respect to high non-controllable demand, planned pump operation is discarded when the tank is full, reduced when available storage would be exceeded, or increased if the water volume stored in the tank drops below the prescribed minimum capacity.

Figures 3 and 4 present the effect of the aforementioned pruning strategy on pump system electricity demand and water tank volume for $\alpha = 0.5$ and the week with higher electricity demand. The previously described direct proportionality of the pump system flow rate and electricity demand is noted. In Figure 4, the proposed pruning strategy is shown to avoid the aforementioned tank overflow throughout the entire week. Moreover, Figure 3 indicates that a substantial weekly household demand and electricity bill portion corresponds to the pump system demand. In addition, to ensure scheduling and tank bound feasibility under significant and less intensive non-controllable water demand, weekly bills are also reduced via the proposed pruning strategy. A similar tank overflow behaviour is also observed for other α weights. This phenomenon is again overcome by considering the aforementioned pump pruning strategy. Finally, given the simplicity of the aforementioned pruning strategy, its real-time implementation is possible and straightforward.

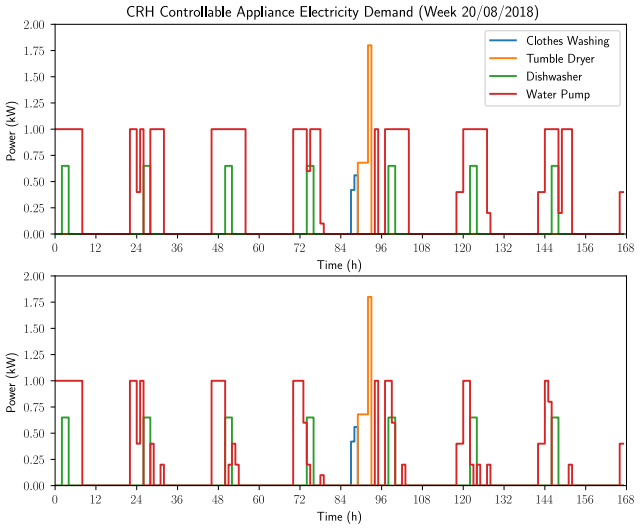

FIGURE 3. Original CRH controllable load demand (top) and after pump system operation pruning (bottom), for $\alpha = 0.5$.

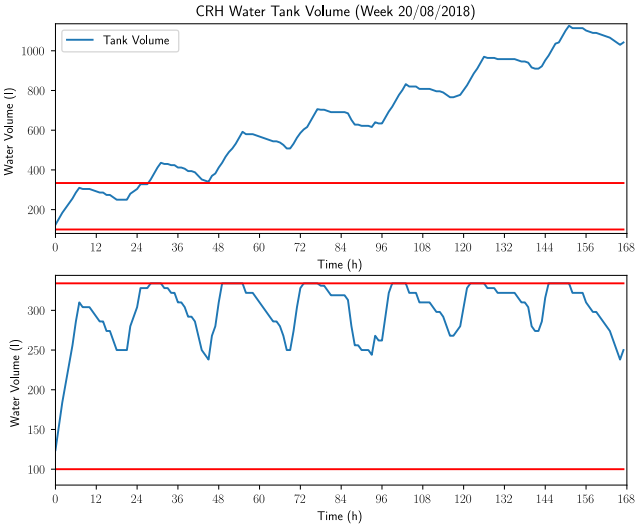

FIGURE 4. Original CRH tank volume (top) and after pump system operation pruning (bottom), for $\alpha = 0.5$.

Compared with what was observed in the case of the water tank, battery system undercharging or overcharging is not detected for any week and α weight. In Figure 5, the battery SOC is presented for the week with higher electricity demand and $\alpha = 0.5$. It can be concluded from Figure 5 that approximately one complete daily battery charge and discharge cycle is carried out. It can also be concluded that nighttime cheaper electricity tariffs are exploited for battery charging. The only exception to this trend is observed on the last day of the week, when the battery is not charged once the minimum SOC is reached. Similar battery system management is observed for different α weights except in the case of $\alpha = 0$, for which micro storage is not exploited and its SOC value remains unchanged and equal to the initial value. The fact that

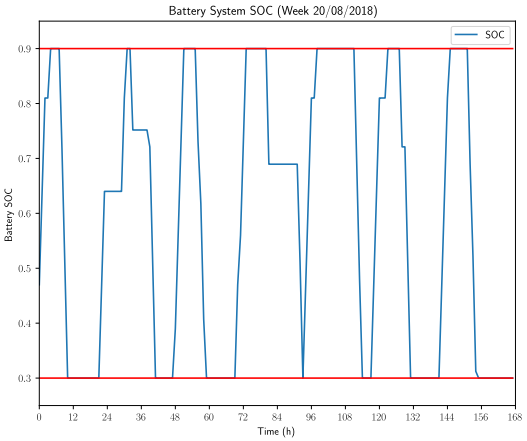

FIGURE 5. Original CRH battery SOC (top) and after pump system operation pruning (bottom), for $\alpha = 0.5$.

resident discomfort is the only criterion considered when $\alpha = 0$ explains the lack of battery use. In this case, scheduling is only concerned with load allocation closer to the preferred operation times. Although the same resident discomfort performance can be obtained using the battery system, solutions with fewer nonzero variables are favoured by the chosen mathematical optimisation solver. Therefore, battery system management reported for $\alpha = 0$ is justified by this reason. A final consideration must be performed, concerning the management of the battery system. For $\alpha > 0$, daily charging and discharging cycles of the battery system are responsible for consistent degradation of this device. Even though, in this paper, it is not intended to analyse the financial viability, or the expected return on investment, of the installation of smart home appliances such as PV panels or battery storage systems, it should be taken into consideration when planning their installation in a smart home environment.

B. TRADITIONAL RECEDING HORIZON

The standard RH-based controllable appliance operation follows the same trends observed for the proposed CRH approach. Afternoon washer and dryer operations and nighttime dishwasher scheduling are observed with $\alpha = 0$ to $\alpha = 0.5$ following resident preferences. Nonetheless, for this α weight range, washer, dryer or dishwasher load starts are delayed by one hour in some weeks relative to the CRH allocation. For $\alpha = 0.75$, weekly washer and dryer loads are more often shifted to nighttime periods, particularly during the first slots of each day. Similarly, in the CRH-based approach, washer and dryer load shifting is conditioned by the underlying contribution of electricity bill minimisation to the objective function of the corresponding optimisation problem instance. For $\alpha = 1$, off-peak controllable appliance operation prevails while overnight washer and tumble dryer operations are more frequent than for the CRH case.

No significant pump system operation or tank volume difference is observed relative to that of CRH. non-controllable nonpotable water demand overestimation is again responsible for excessive pump operation and water tank overflow, such as in the CRH case. Battery system management follows planning trends identified for CRH-based allocation. During all but the last day of the week, a daily battery charge and discharge cycle is executed. The main difference between the CRH and RH approaches is concerned with the last day of the week. Battery charging in the last slots of the seventh day is maintained in RH-based allocation, while battery power consumed during the day is not restored in the CRH approach. Indeed, in the last day of the week, a single-day horizon is considered in the CRH approach, which is inconsistent with the 7-day horizon for the RH case. As such, battery recharging is ensured within an RH framework to account for household electricity demand at the beginning of the next week. Because battery charging takes place at night (off-peak slots), all required power is provided by the grid, which increases the weekly electricity bill.

C. DAY-AHEAD ALLOCATION

The main difference between DA allocation and both CRH and RH is associated with washer and tumble dryer scheduling. For each day of each week, a single-day horizon is specified, in which washer and tumble dryer operations are optional. If washer and dryer scheduling are performed on a given day, then they will not be considered in the following days of the same week. However, washer and dryer allocations on the last day of the week are mandatory if these two appliances have not yet been operated in the course of the underlying week.

First day washer and dryer schedules are observed for all 30 weeks, from $\alpha = 0$ to $\alpha = 0.5$, and this task performed to minimise resident discomfort, which is the criterion with a higher contribution to the problem objective for the aforementioned α weights. Conversely, for $\alpha = \{0.75; 1\}$, maximum washer and dryer deferment is carried out to reduce the electricity bill on individual days. Exceptions in five weeks are identified, for which washer and dryer machines are operated in the first two days of the respective weeks. For dishwasher loads, daily operations from 2 am to 4 am (slots 3 and 4) remain the norm, with few loads anticipated by one slot from 1 am to 3 am (slots 2 and 3).

Concerning the pump system, water tank and battery storage management, operation trends similar to CRH-based scheduling are observed. Predominantly, off-peak pump system operations are noted, which gradually decrease tank inflows as the electricity bill α weight increases. Overall excessive pump operation is verified again, which results in water tank overflow. Similar to CRH and RH, this problem is addressed by discarding excessive pump operations. The battery system is charged during the first hours of each day and subsequently discharged during the daytime. Such behaviour follows CRH and RH schedules. Compared with RH, no battery charging is considered at the end of the last day of the week because the scheduling horizon does not contemplate subsequent days.

D. IDEAL ALLOCATION

In the ideal allocation, knowledge of actual micro power generation, non-controllable electricity and nonpotable water demand is exploited to minimise each weighted criteria combination. Considering that future household demand and generation cannot be predicted in advance with perfect accuracy, the reported ideal allocation performance criteria define lower bounds for each α weight.

Similarly, in previously discussed approaches, controllable allocation follows resident preferences for smaller α to minimise resident discomfort. As α grows, particularly for $\alpha = \{0.75; 1\}$, off-peak washer and dryer shifting is promoted to reduce the electricity bill. For dishwasher loads, their preferred operation times coincide with off-peak tariffs and therefore have remained mostly unchanged.

A similar trend is reported for pump system management. For higher α weights, pump operation is coordinated with washer and non-controllable nonpotable water demand to pump strictly necessary volumes to ensure minimum tank volume satisfaction over the week. Accordingly, electrical pump demand and household electricity bills are minimised while tank volumes are guaranteed to remain within established bounds. In other words, no water tank overflow occurs.

Finally, similar battery storage system management is carried out. In previously discussed approaches, no battery charging or discharging was promoted for $\alpha = 0$. The reasons for battery system operation absence are twofold. First, battery system operation has no impact on resident discomfort, which is the only criterion considered for $\alpha = 0$. Second, because an electricity bill is not considered for $\alpha = 0$, the overall scheduling performance is not further improved by exploiting available storage to reduce grid purchases. With increasing α, more frequent battery usage for domestic supply is observed. Nighttime charging for posterior daytime supply remains the norm for all α other than $\alpha = 0$. When electricity bill minimisation is given a major objective contribution, i.e., for $\alpha = \{0.75; 1\}$, then charging and discharging coordination with household electricity demand and local micro generation is further enhanced. Similarly, for pump system management, only strictly necessary power is directed to battery charging.

E. TYPICAL ALLOCATION

Typical appliance allocation is solely determined by household residents. As such, no electricity bill minimisation α weights are considered. For the residential home considered in this work, controllable appliances are shown to be operated by residents at different times of the day for every day of the 30 weeks. Washer and dryer cycles remain predominantly operated around noon, with few exceptions in some weeks scheduled later in the day, starting at approximately 6 pm. However, dishwasher operation is not shown to follow any concrete pattern. On some days of some weeks, nighttime dishwasher operation was observed, which followed the CRH, RH, DA and ideal allocation operation trends. On other days, a full load of dishes is washed during the day, either at the morning end, noon or afternoon.

Concerning the pump system, its allocation is constrained to specific time periods, which is inconsistent with CRH, RH, DA and even ideal allocation strategies, where the electrical pump system operates throughout the day. In a typical allocation, the water tank is shown to be able to ensure a household nonpotable water supply over a two-day period, after which electrical pump operation is required to refill the tank. As such, approximately three complete tank refills are carried out over one week. The resulting intense electrical pump system operation is mainly carried out at night (off-peak billing), taking advantage of cheaper grid tariffs to mitigate its impact on the weekly electricity bill. Nonetheless, it should be pointed out that refilling the tank can also occur during the daytime (on-peak billing) as long as the minimum tank volume is reached during this period.

For battery storage, similar behaviour to water tank system operation is found, with the main difference related to the battery system charging and discharging frequency. Given that available storage is rather low relative to household electricity needs, several battery charging and discharging cycles are carried out per day, namely, approximately three complete daily charge-discharge cycles.

F. LOAD DEFERMENT ANALYSIS

Similar controllable appliance scheduling solutions are reported for the CRH, RH and DA strategies. Controllable load shifting towards higher resident preference slots is reported for smaller α weights. While the resident discomfort criterion is minimised in this allocation setting, as a side effect, it leads to a higher weekly electricity bill due to washer and dryer load shifting to on-peak slots. Conversely, electricity bill minimisation is favoured for higher α weights, in which controllable loads are allocated to cheaper electricity slots. However, washer and dryer resident preferences are accordingly penalized, with a noticeable impact on resident discomfort criterion performance.

In Figure 6, weekly electricity bill and resident discomfort are presented for all five α weights for the week with maximum electricity demand. Because typical appliance allocations are directly retrieved from historical records, the performance of typical allocation with respect to weekly electricity bill and resident discomfort is not affected by each particular α weight considered. Typical appliance operation performance is, nonetheless, presented for each α weight for easier comparison against the other strategies. In Figure 6, a trade-off between weekly electricity bills and resident discomfort is shown. For the considered week, no significant resident discomfort variation is observed as a function of α weights and scheduling approaches, including the ideal allocation setting. The reason for the observed similar resident discomfort performance can be explained by the resident discomfort criterion, which is only influenced by the slot of the day in which washer, dryer and dishwasher loads are operated. Indeed, according to the specification

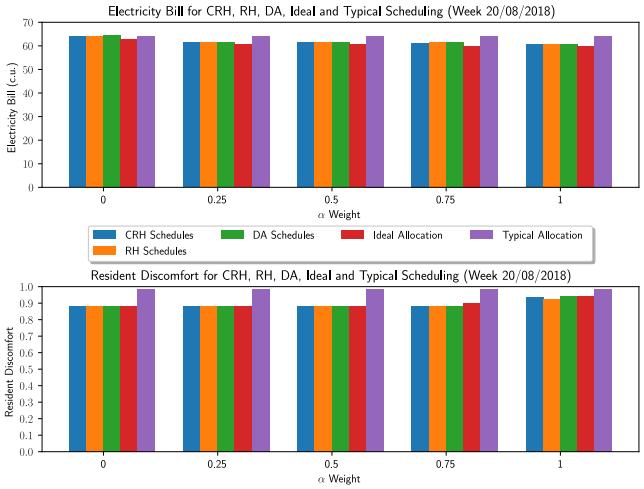

FIGURE 6. Electricity bill (top) and resident discomfort (bottom) evaluated for all approaches and α weights in the week with maximum electricity demand.

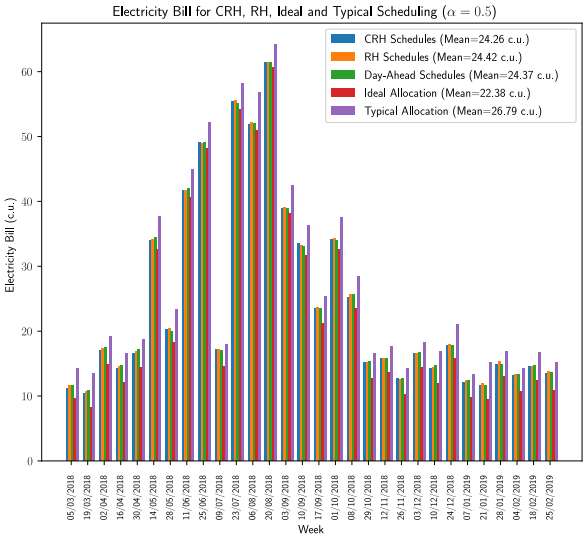

FIGURE 7. Electricity bill for CRH, RH, DA and ideal scheduling over the 30 weeks, considering $\alpha = 0.5$.

of this criterion in (2), scheduling the same appliance to the same slots of the day across different days results in the same resident discomfort. As presented in Sections V-A, V-B and V-C, the three abovementioned appliances remain scheduled mostly to the same slots of the day under the same α parametrisation. However, for certain days of some weeks, individual loads of any one of these appliances may be anticipated or delayed by up to two slots; thus, small variations of the corresponding resident operation preference are often observed, which justifies the observed resident discomfort criterion performance similarities.

Concerning weekly electricity bills, the CRH, RH and DA scheduling approaches are shown to be farther from the ideal allocation performance, particularly for $\alpha = 0$. All optimisation-based approaches, namely, CRH, RH, DA and ideal allocation, are shown to outperform the typical allocation whenever electricity bill minimisation is considered, i.e., $\alpha = \{0.25; 0.5; 0.75; 1\}$. However, when only resident discomfort minimisation is considered, i.e., $\alpha = 0$, the typical allocation is shown to match other strategies in terms of weekly electricity bills.

Typical appliance allocation scores lead to worse resident discomfort performance among all strategies under consideration, even when this criterion is not taken into account in daily optimisation problem instances, i.e., for $\alpha = 1$. As previously argued, historical appliance usage records collected for those 30 weeks show no clear operation pattern for the washer, dryer or dishwasher. Moreover, the absence of preferred operation time information for the selected household motivated the estimation of these periods from the available one-year historical records. The implications of no clear appliance operation patterns and the absence of preferred operation time information are twofold: (i) if no clear operation pattern is identified, then the estimation procedure proposed in [26] results in multiple day slots with higher preference. As each appliance is only operated during a few slots in the day, an overall high resident discomfort value is inevitably obtained. (ii) The observed appliance operation over each of the 30 weeks may not correspond to a preferred operation setting. Indeed, observed load scheduling could be due to suboptimal choices made by residents, with no intention of minimising discomfort. Moreover, some of these loads could have also been scheduled at higher discomfort periods due to unexpected events, such as late home arrival after work.

The absence of resident preference motivated a trade-off between electricity bill and resident discomfort by setting $\alpha = 0.5$. It should be mentioned at this point that in real-world scenarios, inquiries should be submitted to household residents so that a reliable α weight can be selected.

Figures 7 and 8 present the electricity bill and resident discomfort for CRH, RH, DA, ideal and typical allocation over the 30 weeks, respectively, assuming $\alpha = 0.5$. In the supplemental material accompanying this document, planned washer, dryer and dishwasher appliance operations obtained from CRH, RH, DA, ideal scheduling and typical allocation is shown for each week and $\alpha = 0.5$. The average weekly electricity bill over the 30 weeks is 24.26 c.u. for CRH, 24.42 c.u. for RH, 24.37 c.u. for DA, 22.38 c.u. for ideal allocation, and 26.79 c.u. for typical appliance operation. Regarding the average resident discomfort over the 30 weeks, all scheduling approaches scored 0.88, except typical appliance operations, which scored an average discomfort of 0.96.

For the chosen α, the typical appliance allocation is consistently outperformed by all the other strategies, according to both weekly electricity bill and resident discomfort. Conversely, the ideal allocation is shown to outperform its counterparts in terms of electricity bills in each of the 30 weeks. For the CRH, RH and DA approaches, no one

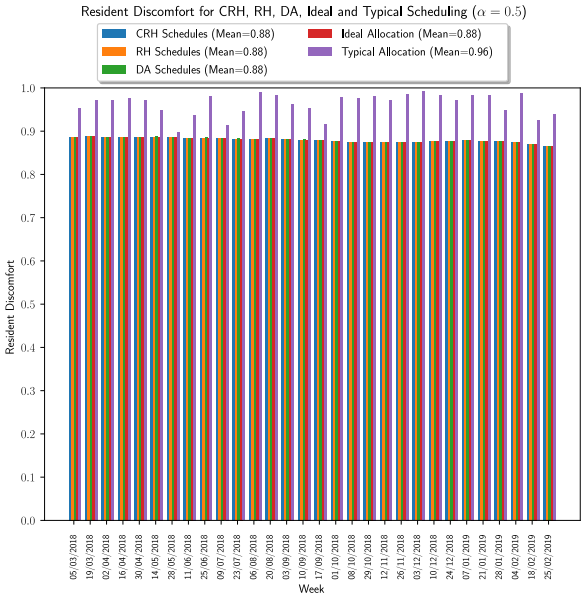

FIGURE 8. Resident discomfort for CRH, RH, DA and ideal scheduling over the 30 weeks, considering $\alpha = 0.5$.

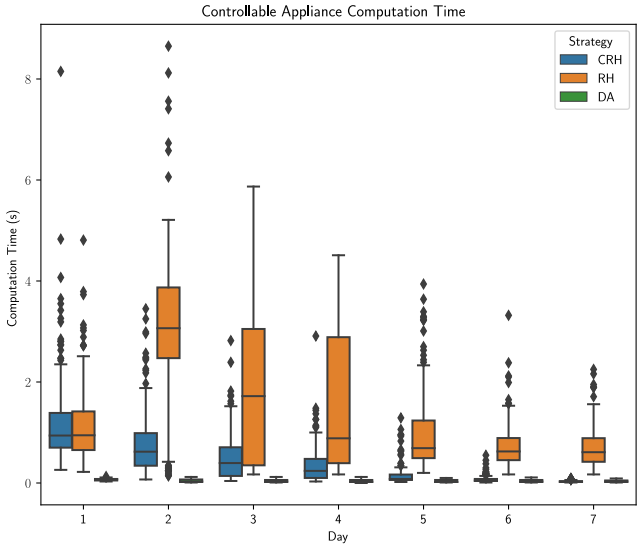

FIGURE 9. Controllable appliance computation time for each horizon day.

is shown to consistently outperform the others, according to both weekly electricity bill and resident discomfort. Moreover, in the case of resident discomfort, no difference is found between any of the three abovementioned strategies in any of the 30 weeks. However, slight differences in weekly electricity bill scores based on CRH, RH and DA scheduling are noticed over the 30 weeks. A lower average weekly electricity bill is shown for the proposed CRH approach, although by a small amount. For all 30 weeks, the maximum electricity bill savings resulting from CRH-based allocation did not exceed 0.16 currency units compared with RH and DA.

In addition to the weekly electricity bill and resident discomfort performance, the computational burden is also investigated. In Figure 9, CRH, RH and DA computation time is presented in box-and-whisker plots for each horizon day and all five α weights. Controllable appliance allocation is shown to be carried out very fast, in a matter of a few seconds, on any horizon day. DA allocation stands out from its CRH and RH counterparts, with the controllable appliance scheduling solution found almost instantly on any horizon day. In the case of CRH-based allocation, as progressively shorter scheduling horizons are considered, the computation time is observed to decrease as the week advances until it matches that of DA. Finally, an overall higher computation time is obtained for the standard RH allocation, which can be expected to some extent because longer scheduling horizons are considered.

In the prototypical smart home case study considered, daily appliance allocation is carried out in the last slot of the day that precedes the first day of the horizon. Given the hourly time slots considered in this work, a 1 h computation time limit is imposed for daily appliance allocation. As can be inferred from Figure 9, estimating representative demand profiles, retrieving micro PV generation forecasts and solving the corresponding MILP optimisation problem instance are carried out in a matter of a few seconds. As such, the 1 h computation time limit imposed for daily appliance allocation is respected and controllable schedules are available to be implemented at the start of each horizon. However, it is observed from simulation results that CRH allocation presents a comparable performance to that shown by RH and DA allocations. As discussed in Sections V-A to V-C, for the same α weights, controllable appliances are operated during approximately the same slots, and similar battery and pump system management is reported. As such, very close electricity bill and resident discomfort performance is shown for all the scheduling strategies under the same week and α criterion weight.

Figures 10 and 11 present the cumulative weekly electricity bill and resident discomfort difference histogram between CRH and the ideal allocation for all α weights, respectively. Coloured horizontal and vertical lines are drawn for the 90^{th} percentile of the bill and resident discomfort difference distributions. In 90% of the simulations, the CRH-based weekly electricity bill is shown to not exceed the ideal scenario by more than 2.54 currency unit. Considering that future demand and generation cannot be perfectly predicted in any real-world scenario, the gap to the ideal allocation weekly electricity bill can be considered acceptable. Concerning resident discomfort, a tiny difference from the ideal performance is observed, with CRH-based allocation not surpassing the ideal allocation resident discomfort by more than 0.013 in 90% of the simulations.

Taking into account the simulation results, the novel CRH proposal shows a competitive performance relative to that of the standard RH and DA strategies. A discomfort score similar to that of the ideal scenario is also observed along with an acceptable gap to the ideal electricity bill. Moreover,

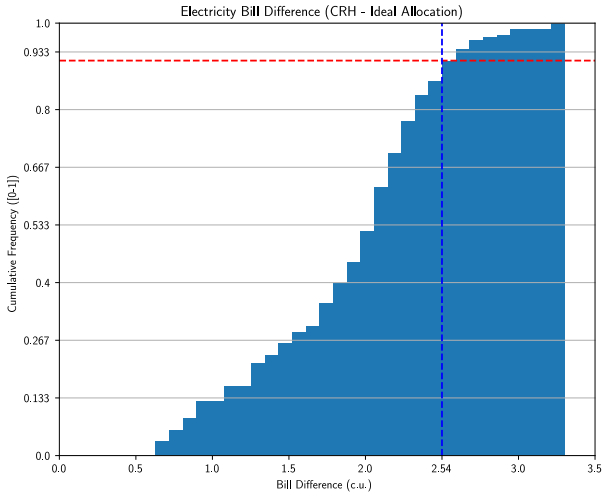

FIGURE 10. Histogram of the cumulative electricity bill difference between CRH and ideal scheduling.

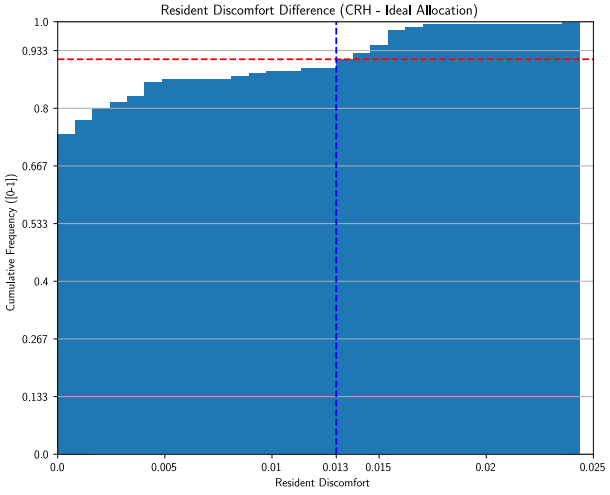

FIGURE 11. Histogram of the cumulative resident discomfort difference between CRH and ideal schedules.

relative to the typical appliance operation, the novel CRH approach is reported to achieve a noticeable improvement in both weekly electricity bill and resident discomfort performance. The fact that the allocation of appliances not required to operate every day is considered across different horizons before a decision is made is an intrinsic advantage of the CRH framework. Accordingly, updated PV generation forecasts are inherently taken into account in the selection of the most beneficial slot allocation, thereby reducing grid demand stress and weekly electricity bills. In short, the proposed CRH approach is shown to be capable of satisfying the same electricity needs with overall smaller grid demand stress. This is critical for entities responsible for managing the grid infrastructure, particularly if carried out at a large scale. In addition, fewer and less frequent expensive interventions aimed at expanding both the generation and transmission capacity of the power grid will be required. Carbon emissions and other negative environmental impacts stemming from fossil fuel exploitation are concomitantly addressed.

VI. CONCLUSION

This work addressed the problem of week-ahead household appliance scheduling. A CRH-based approach was proposed to address the misalignment of DA and RH scheduling strategies with weekly household appliance usage patterns. Scheduling was carried out for 30 different weeks over a one-year period. A prototypical smart home equipped with PV panels, a battery system, and representing a possible real-world scenario for a family of four residents was considered. Electricity and nonpotable water demand were modelled by historical real-world data and probability distributions. Similar scheduling performance is registered for the three evaluated strategies, namely, CRH, RH and DA allocation. Off-peak allocation was predominant, particularly for higher weekly electricity bill contributions, corresponding to larger α values. Simulation results validated the proposed CRH approach in week-ahead household appliance scheduling. The novel strategy showed competitive performance that aligned with that recorded for standard RH and DA scheduling methods available in the literature; therefore, it represents a valid alternative to RH and DA-based scheduling. Compared with a typical appliance operation, improvements in terms of both weekly electricity bill and resident discomfort were shown for the CRH strategy. Finally, near-ideal CRH performance with negligible comfort impact and acceptable weekly electricity bill gap was noticed. Directions for future work include assessing the proposed CRH approach in different smart home scenarios, with higher micro PV generation output and explicit non-controllable demand and generation modelling, via stochastic or robust programming. Further research into automatic and intelligent discovery of preferred appliance operation times could also be carried out, as in other literature works. Finally, degradation costs resulting from battery system charging and discharging, and micro PV generation output losses, due to PV panel discolouration, can also be considered as additional objectives. By doing so, further adjustments on planned controllable appliance operation can be carried out, in order to maximise the longevity of smart home devices.

APPENDIX

A COMPRESSIVE RECEDING HORIZON APPROACH FOR SMART HOME ENERGY MANAGEMENT—SUPPLEMENTAL MATERIAL

In the following, supplemental material is presented and organised as follows. Section A derives the lower and upper bounds for the electricity bill appliance scheduling criterion. Section B derives the lower and upper bounds for the resident discomfort appliance scheduling criterion. Finally, Section C presents the controllable appliance schedules for each of the 30 weeks planned for electricity bill minimisation weight $\alpha = 0.5$ with each strategy considered.

A. HOUSEHOLD ELECTRICITY BILL CRITERION BOUNDS

1) HOUSEHOLD ELECTRICITY BILL LOWER BOUND

Taking into consideration decision variables $w_i, t_i, d_i, q_i, sw_i, st_i$, $i = 1, \ldots, T$, parameters p_d^{full}, p_p^{full}, p_w^{full}, p_w^{last}, p_t^{full} and p_t^{last}, a domestic electricity balance lower bound is derived. Let ω, Λ_i and Υ_i, $i = 1, \ldots, T$ be defined in (23).

$$\begin{aligned}\omega &= \frac{q_{min}}{q_{max}} p_p^{full} + p_{min}^{bc} - p_{max}^{bd} \\ \Lambda_i &= d_i\, p_d^{full} + \frac{q_i}{q_{max}} p_p^{full} + w_i\, p_w^{full} \\ &\quad + sw_{(i-l_w+1)} \left(p_w^{last} - p_w^{full}\right) \\ &\quad + t_i\, p_t^{full} + st_{(i-l_t+1)} \left(p_t^{last} - p_t^{full}\right) \\ \Upsilon_i &= p_i^{bc} - p_i^{bd} - PV_i \quad i = 1, \ldots, T \end{aligned} \tag{23}$$

Considering $w_i, t_i, d_i, sw_i, st_i \in \{0, 1\}$, $i = 1, \ldots, T$, bounds on variables q_i imposed in (7) for $i = 1, \ldots, T$, and bounds on variables p_i^{bc} and p_i^{bd} imposed in (20) for $i = 1, \ldots, T$, the weekly electricity bill lower bound is derived in (24) for each horizon slot i, $i = 1, \ldots, T$.

$$\begin{aligned}\Lambda_i &\geq \frac{q_{min}}{q_{max}} p_p^{full} \\ &\Leftrightarrow \Lambda_i + E_i^{home} \geq \frac{q_{min}}{q_{max}} p_p^{full} + E_i^{home} \\ &\Leftrightarrow \Lambda_i + E_i^{home} + \Upsilon_i \geq E_i^{home} + \omega - PV_i \\ &\Leftrightarrow e_i \geq E_i^{home} + \omega - PV_i \quad i = 1, \ldots, T \end{aligned} \tag{24}$$

where $\Lambda_i + E_i^{home} + \Upsilon_i = e_i$ from (6). Considering $B_i > S$, $\forall\, i = 1, \ldots, T$ the weekly electricity bill lower bound is further derived in (25).

$$\begin{aligned}\sum_{i=1}^{T} \left(B_i e_i^+ - S e_i^-\right) &\geq \sum_{i=1}^{T} \left(S e_i^+ - S e_i^-\right) \\ &\Leftrightarrow \sum_{i=1}^{T} \left(B_i e_i^+ - S e_i^-\right) \geq \sum_{i=1}^{T} S \left(e_i^+ - e_i^-\right) \\ &\Leftrightarrow \sum_{i=1}^{T} \left(B_i e_i^+ - S e_i^-\right) \geq S \sum_{i=1}^{T} e_i \end{aligned} \tag{25}$$

Considering the lower bound derived in (24), the expression in (25) is further extended in (26).

$$\sum_{i=1}^{T} \left(B_i e_i^+ - S e_i^-\right) \geq S \sum_{i=1}^{T} e_i \geq EB_{min} \tag{26}$$

where $EB_{min} = S \sum_{i=1}^{T} \left(E_i^{home} - PV_i + \omega\right)$ is a lower bound on weekly electricity bills, with $\omega = \frac{q_{min}}{q_{max}} p_p^{full} + p_{min}^{bc} - p_{max}^{bd}$.

2) HOUSEHOLD ELECTRICITY BILL UPPER BOUND

Recalling the nature of decision variables $w_i, t_i, d_i, q_i, sw_i, st_i$, for $i = 1, \ldots, T$, parameters p_d^{full}, p_p^{full}, p_w^{full}, p_w^{last}, p_t^{full} and p_t^{last}, and Υ_i defined in (23), for $i = 1, \ldots, T$, let Ω be defined in (27).

$$\Omega = p_d^{full} + p_p^{full} + p_w^{full} + p_t^{full} + p_{max}^{bc} - p_{min}^{bd} \tag{27}$$

Based on the aforementioned problem parameters, variables and constraints, an upper bound on domestic electricity balance at any slot i of the horizon for $i = 1, \ldots, T$ is derived in (28).

$$\begin{aligned}\Lambda_i &\leq p_d^{full} + p_p^{full} + p_w^{full} + p_t^{full} \\ &\Leftrightarrow \Lambda_i + E_i^{home} \leq p_d^{full} + p_p^{full} + p_w^{full} + p_t^{full} + E_i^{home} \\ &\Leftrightarrow \Lambda_i + E_i^{home} + \Upsilon_i \leq \Omega + E_i^{home} - PV_i \\ &\Leftrightarrow e_i \leq \Omega + E_i^{home} - PV_i \quad i = 1, \ldots, T \end{aligned} \tag{28}$$

Revisiting the household electricity bill defined in (2) and household electricity balance constraints in (5), it follows that the maximum weekly electricity bill occurs when $e_i^- = 0$, implying $e_i^+ = e_i$. Moreover, from (5), $e_i^+ \geq 0$ resulting in $e_i \geq 0$. Therefore, the expression in (28) is further developed in (29).

$$0 \leq e_i \leq \Omega + E_i^{home} - PV_i \tag{29}$$

Finally, the household electricity bill upper bound is defined in (30).

$$\begin{aligned}&\sum_{i=1}^{T} \left(B_i e_i^+ - S e_i^-\right) \leq \sum_{i=1}^{T} B_i e_i \\ \Leftrightarrow &\sum_{i=1}^{T} \left(B_i e_i^+ - S e_i^-\right) \leq \sum_{i=1}^{T} B_i \left(\Omega + E_i^{home} - PV_i\right) \end{aligned} \tag{30}$$

where $EB_{max} = \sum_{i=1}^{T} B_i \left(\Omega + E_i^{home} - PV_i\right)$ is an upper bound on the household electricity bill.

B. HOUSEHOLD RESIDENT DISCOMFORT CRITERION BOUNDS

The RD criterion is defined in (2), where weight equality $\varrho_w = \varrho_t = \varrho_d = \frac{1}{3}$ is noted. Moreover, the adopted method to determine household resident preference vectors guarantees that $\sum_{i=1}^{h} \zeta_i^{\mathrm{w}} = \sum_{i=1}^{h} \zeta_i^{\mathrm{t}} = \sum_{i=1}^{h} \zeta_i^{\mathrm{d}} = 1$. The lower and upper bounds on household resident discomfort considering only washing machine operations are derived in (31).

$$\begin{aligned}&0 \leq \sum_{i=1}^{h} \zeta_i^{\mathrm{w}} \leq 1, \quad i = 1, \ldots, h \\ \Leftrightarrow\ &0 \leq \sum_{d_g=d_0}^{d_f} \sum_{i=1}^{h} \zeta_i^{\mathrm{w}} \leq \left(d_f - d_0 + 1\right) \\ \Leftrightarrow\ &0 \leq \sum_{d_g=d_0}^{d_f} \sum_{i=1}^{h} \zeta_i^{\mathrm{w}}\, w_{(d_g-d_0)\,h+i} \leq \left(d_f - d_0 + 1\right) \\ \Leftrightarrow\ &0 \leq \frac{\sum_{d_g=d_0}^{d_f} \sum_{i=1}^{h} \zeta_i^{\mathrm{w}}\, w_{(d_g-d_0)\,h+i}}{\sum_{d_g=d_0}^{d_f} \sum_{i=1}^{h} \zeta_i^{\mathrm{w}}} \leq 1 \end{aligned} \tag{31}$$

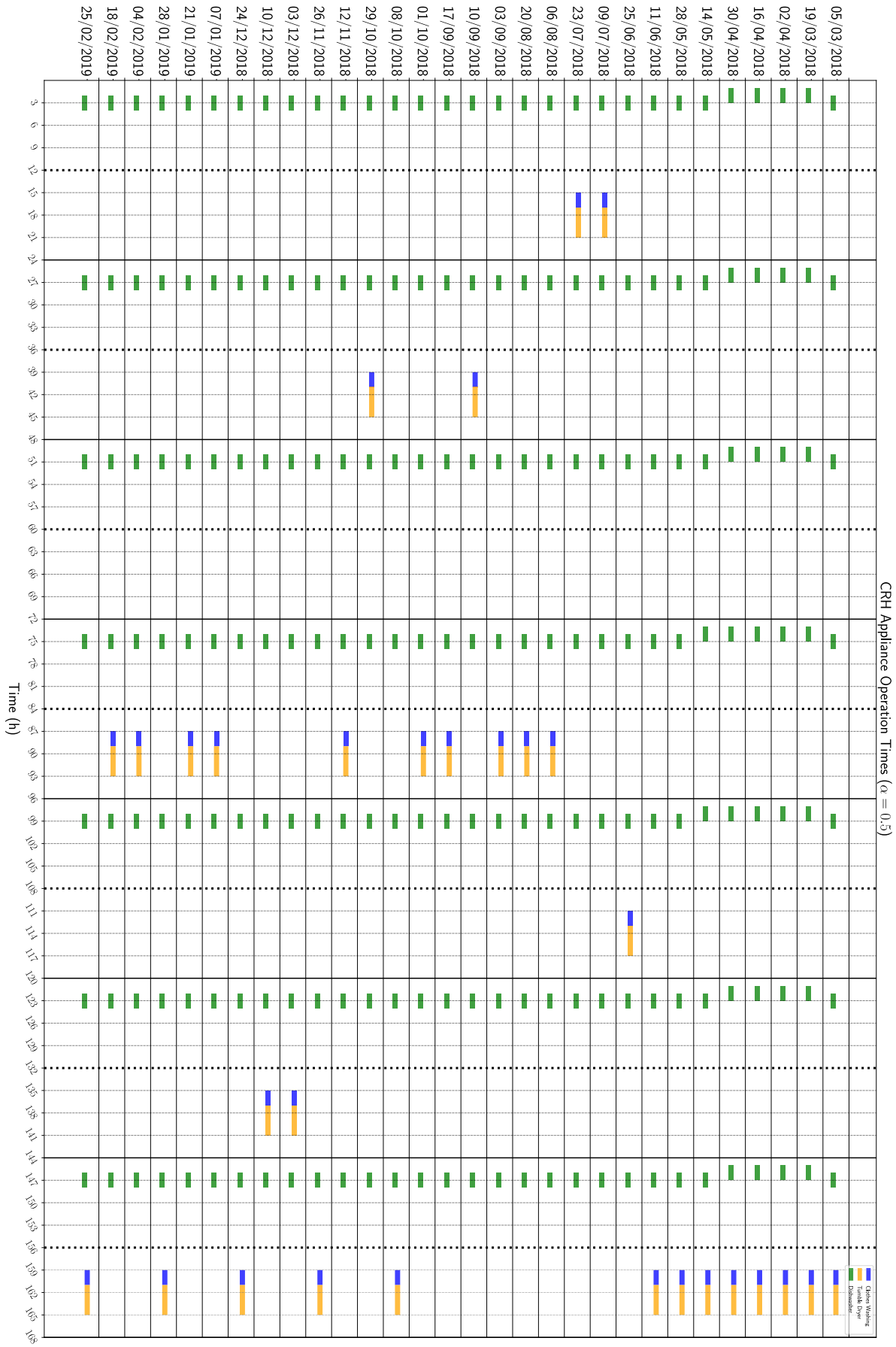

FIGURE 12. CRH-based washer, dryer and dishwasher schedules over the 30 weeks for $\alpha = 0.5$.

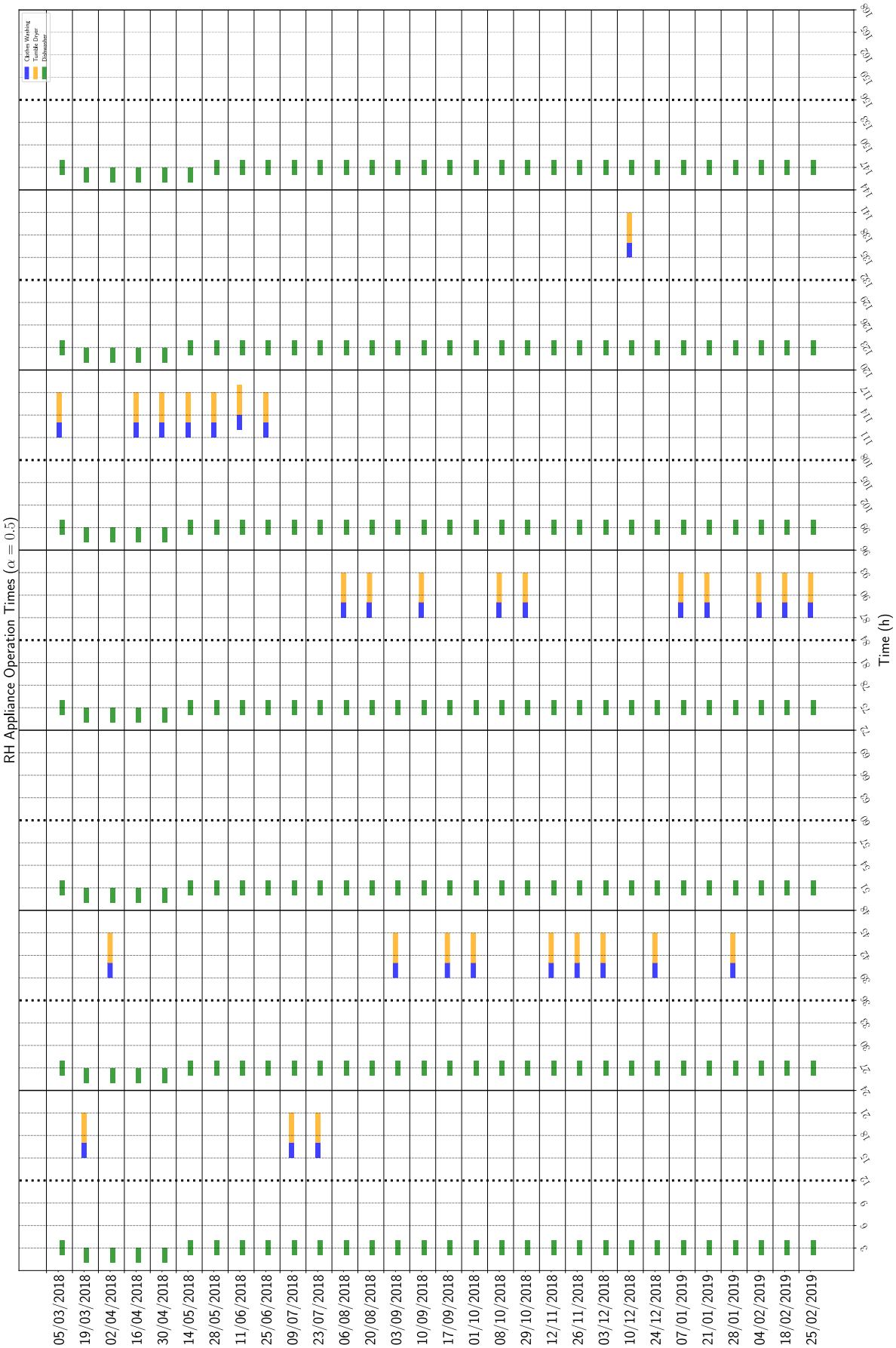

FIGURE 13. RH-based washer, dryer and dishwasher schedules over the 30 weeks for $\alpha = 0.5$.

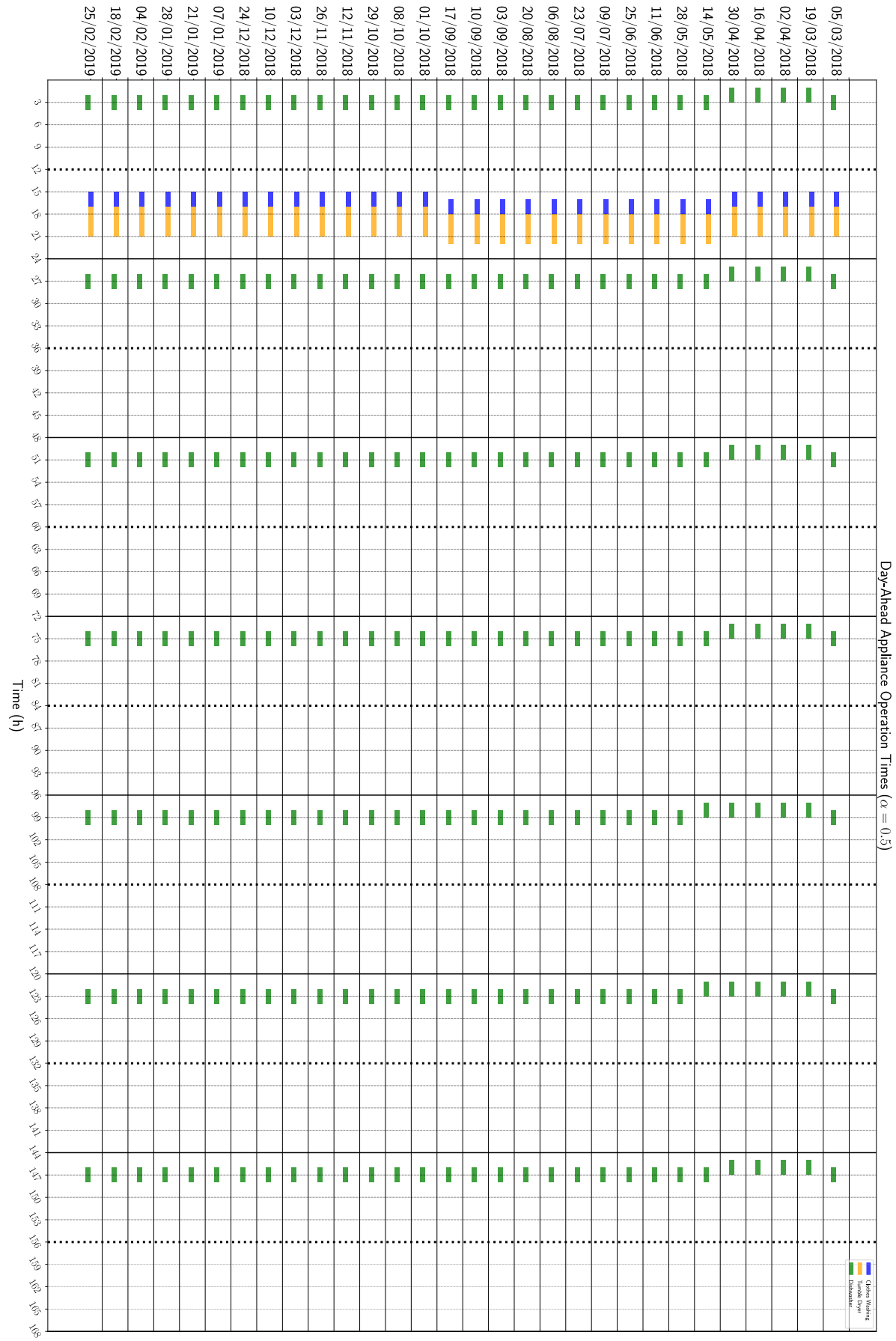

FIGURE 14. DA-based washer, dryer and dishwasher schedules over the 30 weeks for $\alpha = 0.5$.

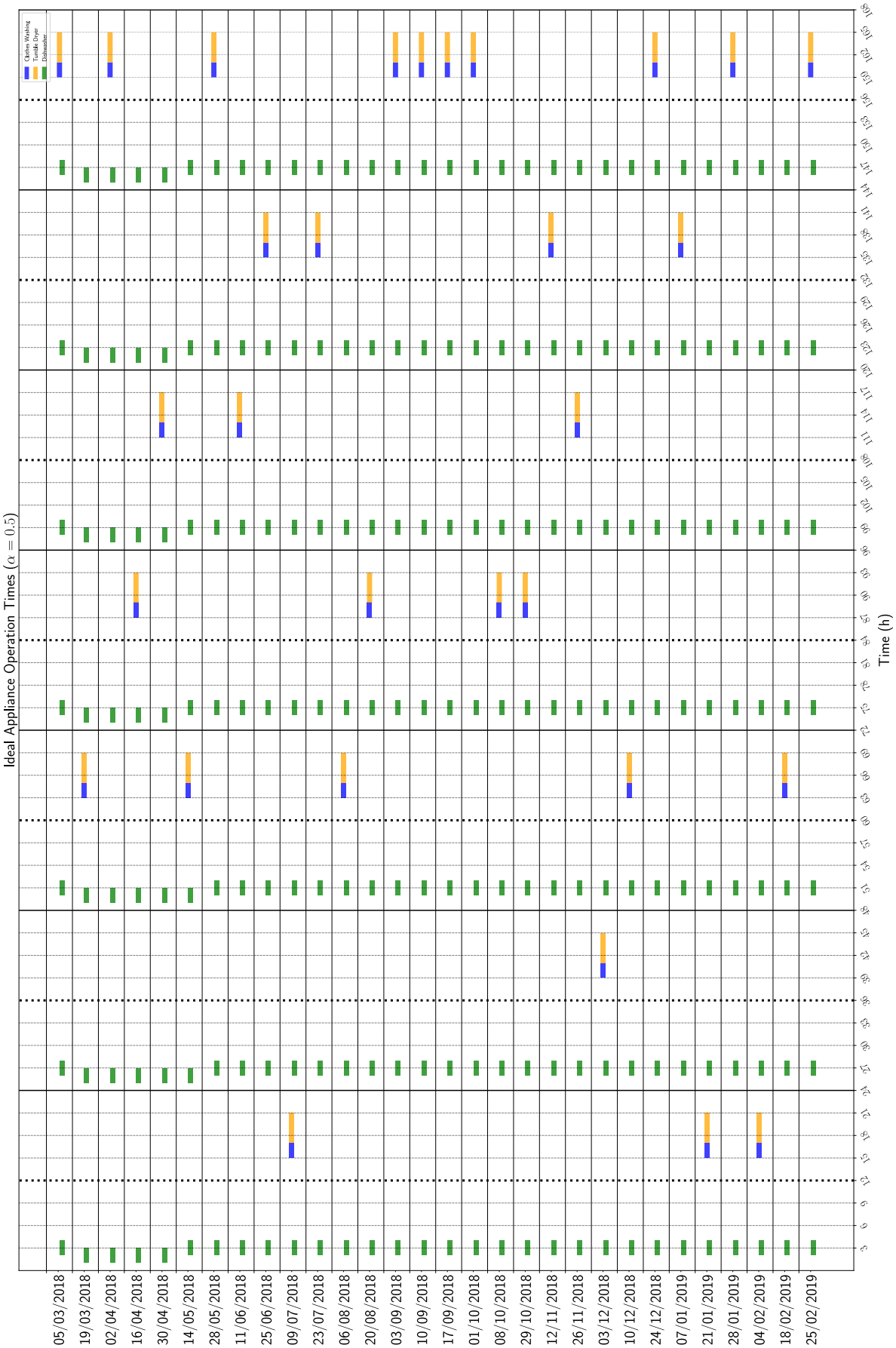

FIGURE 15. Ideal washer, dryer and dishwasher schedules over the 30 weeks for $\alpha = 0.5$.

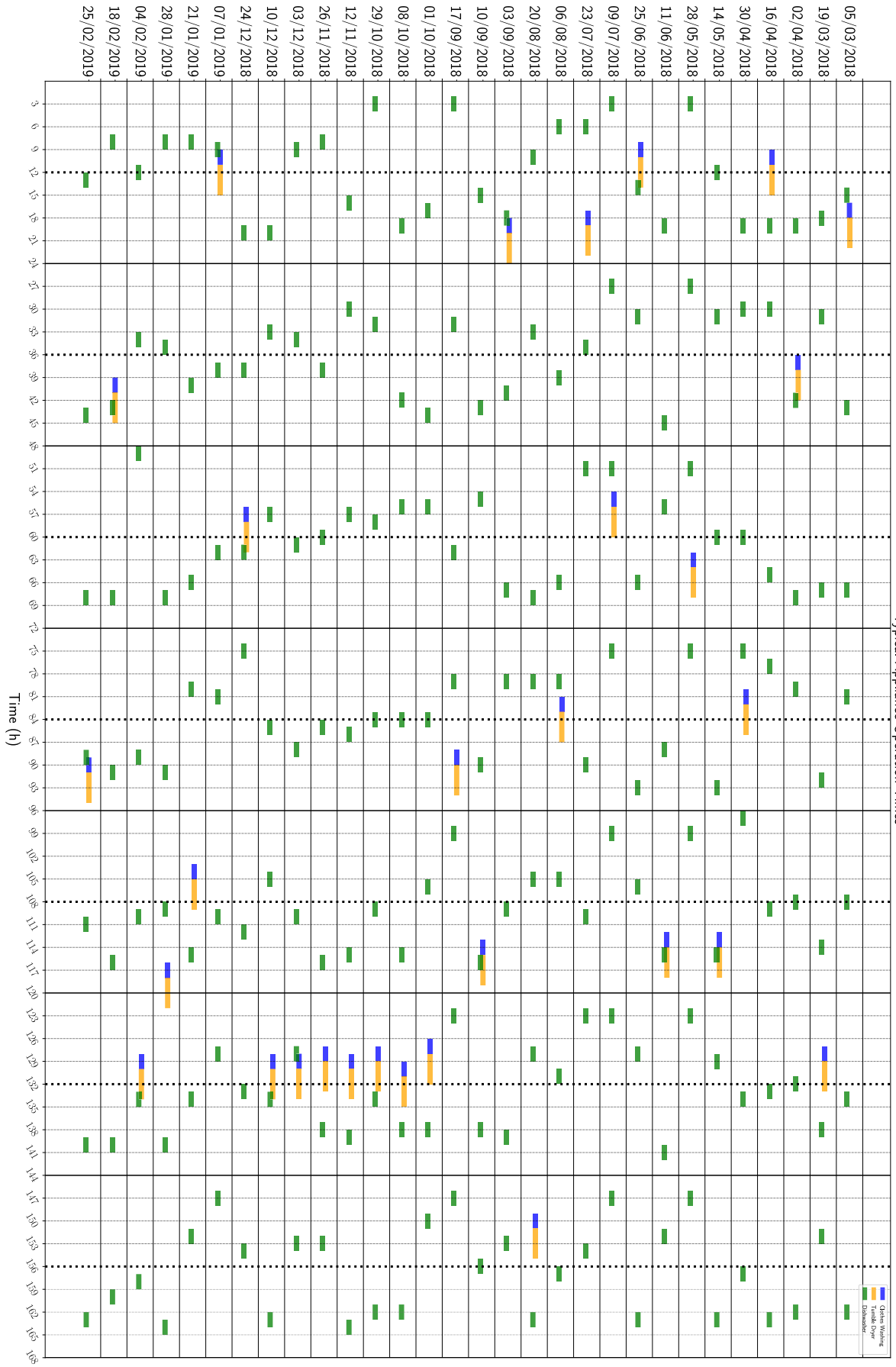

FIGURE 16. Typical washer, dryer and dishwasher schedules over the 30 weeks.

Considering the property $\sum_{i=1}^{h} \zeta_i^{\mathrm{w}} = 1, \sum_{d_g=d_0}^{d_f} \sum_{i=1}^{h} \zeta_i^{\mathrm{w}}$, then $\sum_{d_g=d_0}^{d_f} \sum_{i=1}^{h} \zeta_i^{\mathrm{w}} = \sum_{d_g=d_0}^{d_f} 1 = (d_f - d_0 + 1)$. As such, $\sum_{d_g=d_0}^{d_f} \sum_{i=1}^{h} \zeta_i^{\mathrm{w}} \neq 0$ makes the fraction in the last expression of (31) defined for any $\zeta_i^{\mathrm{w}}, i = 1, \ldots, h$. Building upon these results, the expression in (31) is further developed in (32).

$$
\begin{aligned}
0 \leq & \frac{\sum_{d_g=d_0}^{d_f} \sum_{i=1}^{h} \zeta_i^{\mathrm{w}} \, w_{(d_g-d_0)\,h+i}}{(d_f - d_0 + 1) \sum_{i=1}^{h} \zeta_i^{\mathrm{w}}} \leq 1 \\
\Leftrightarrow 0 \leq & \, \varrho_w \frac{\sum_{d_g=d_0}^{d_f} \sum_{i=1}^{h} \zeta_i^{\mathrm{w}} \, w_{(d_g-d_0)\,h+i}}{(d_f - d_0 + 1)} \leq \frac{1}{3} \\
\Leftrightarrow -\frac{1}{3} \leq & -\varrho_w \frac{\sum_{d_g=d_0}^{d_f} \sum_{i=1}^{h} \zeta_i^{\mathrm{w}} \, w_{(d_g-d_0)\,h+i}}{(d_f - d_0 + 1)} \leq 0
\end{aligned} \tag{32}
$$

The same rationale presented in (31) and (32) can be further extended to the dryer and dishwasher, resulting in (33).

$$
-\frac{1}{3} \leq -\varrho_t \frac{\sum_{d_g=d_0}^{d_f} \sum_{i=1}^{h} \zeta_i^{\mathrm{t}} \, t_{(d_g-d_0)\,h+i}}{(d_f - d_0 + 1)} \leq 0 \tag{33}
$$

$$
-\frac{1}{3} \leq -\varrho_d \frac{\sum_{d_g=d_0}^{d_f} \sum_{i=1}^{h} \zeta_i^{\mathrm{d}} \, d_{(d_g-d_0)\,h+i}}{(d_f - d_0 + 1)} \leq 0 \tag{34}
$$

Finally, adopting the notation introduced in (35),

$$
\begin{aligned}
RD_w &= \varrho_w \sum_{d_g=d_0}^{d_f} \sum_{i=1}^{h} \zeta_i^{\mathrm{w}} \, w_{(d_g-d_0)\,h+i} \\
RD_t &= \varrho_t \sum_{d_g=d_0}^{d_f} \sum_{i=1}^{h} \zeta_i^{\mathrm{t}} \, t_{(d_g-d_0)\,h+i} \\
RD_d &= \varrho_d \sum_{d_g=d_0}^{d_f} \sum_{i=1}^{h} \zeta_i^{\mathrm{d}} \, d_{(d_g-d_0)\,h+i}
\end{aligned} \tag{35}
$$

the expression in (32) is further developed in (36).

$$
\begin{aligned}
-1 \leq & -\frac{RD_w}{d_f - d_0 + 1} - \frac{RD_t}{d_f - d_0 + 1} - \frac{RD_d}{d_f - d_0 + 1} \leq 0 \\
\Leftrightarrow -1 \leq & -\frac{RD_w + RD_t + RD_d}{d_f - d_0 + 1} \leq 0 \\
\Leftrightarrow 0 \leq & \, 1 - \frac{RD_w + RD_t + RD_d}{d_f - d_0 + 1} \leq 1 \Leftrightarrow
\end{aligned} \tag{36}
$$

The resident discomfort criterion is, therefore, shown to be restricted to the [0, 1] interval. As such, no normalisation is required.

C. CONTROLLABLE APPLIANCE SCHEDULING

Figures 12 to 16 present appliance schedules for the washer, dryer and dishwasher over the 30 weeks considered, planned via (i) the novel CRH proposal, (ii) traditional RH, (iii) DA, (iv) ideal scheduling, and (v) typical allocation. Presented controllable appliance schedules are determined for electricity bill minimisation weight $\alpha = 0.5$.

REFERENCES

[1] L. Xu, L. Hou, Z. Zhu, Y. Li, J. Liu, T. Lei, and X. Wu, "Mid-term prediction of electrical energy consumption for crude oil pipelines using a hybrid algorithm of support vector machine and genetic algorithm," *Energy*, vol. 222, May 2021, Art. no. 119955. [Online]. Available: https://www.sciencedirect.com/science/article/pii/S0360544221002048

[2] R. Figueiredo, P. Nunes, M. J. N. O. Panão, and M. C. Brito, "Country residential building stock electricity demand in future climate—Portuguese case study," *Energy Buildings*, vol. 209, Feb. 2020, Art. no. 109694. [Online]. Available: http://www.sciencedirect.com/science/article/pii/S0378778819313908

[3] J. Leitao, P. Gil, B. Ribeiro, and A. Cardoso, "A survey on home energy management," *IEEE Access*, vol. 8, pp. 5699–5722, 2020.

[4] C.-L. Liao, S.-J. Lee, Y.-S. Chiou, C.-R. Lee, and C.-H. Lee, "Power consumption minimization by distributive particle swarm optimization for luminance control and its parallel implementations," *Expert Syst. Appl.*, vol. 96, pp. 479–491, Apr. 2018.

[5] Y.-H. Lin and Y.-C. Hu, "Residential consumer-centric demand-side management based on energy disaggregation-piloting constrained swarm intelligence: Towards edge computing," *Sensors*, vol. 18, no. 5, p. 1365, Apr. 2018. [Online]. Available:https://www.mdpi.com/1424-8220/18/5/1365

[6] Y.-Y. Chen, M.-H. Chen, C.-M. Chang, F.-S. Chang, and Y.-H. Lin, "A smart home energy management system using two-stage non-intrusive appliance load monitoring over fog-cloud analytics based on Tridium's Niagara framework for residential demand-side management," *Sensors*, vol. 21, no. 8, p. 2883, Apr. 2021. [Online]. Available:https://www.mdpi.com/1424-8220/21/8/2883

[7] S. Hussain, C. Z. El-Bayeh, C. Lai, and U. Eicker, "Multi-level energy management systems toward a smarter grid: A review," *IEEE Access*, vol. 9, pp. 71994–72016, 2021.

[8] M. M. Iqbal, M. F. Zia, K. Beddiar, and M. Benbouzid, "Optimal scheduling of grid transactive home demand responsive appliances using polar bear optimization algorithm," *IEEE Access*, vol. 8, pp. 222285–222296, 2020.

[9] O. Alıç and Ü. B. Filik, "A multi-objective home energy management system for explicit cost-comfort analysis considering appliance category-based discomfort models and demand response programs," *Energy Buildings*, vol. 240, Jun. 2021, Art. no. 110868. [Online]. Available: https://www.sciencedirect.com/science/article/pii/S0378778821001523

[10] Z. Yahia and A. Pradhan, "Multi-objective optimization of household appliance scheduling problem considering consumer preference and peak load reduction," *Sustain. Cities Soc.*, vol. 55, Apr. 2020, Art. no. 102058. [Online]. Available: http://www.sciencedirect.com/science/article/pii/S2210670720300457

[11] I. Hammou Ou Ali, M. Ouassaid, and M. Maaroufi, "Day ahead appliance scheduling with renewable energy integration for smart homes," in *Proc. IEEE Int. Autumn Meeting Power, Electron. Comput. (ROPEC)*, Nov. 2020, pp. 1–6.

[12] S. Nan, M. Zhou, G. Li, and Y. Xia, "Optimal scheduling approach on smart residential community considering residential load uncertainties," *J. Electr. Eng. Technol.*, vol. 14, no. 2, pp. 613–625, Mar. 2019.

[13] M. S. Javadi, M. Gough, M. Lotfi, A. E. Nezhad, S. F. Santos, and J. P. S. Catalão, "Optimal self-scheduling of home energy management system in the presence of photovoltaic power generation and batteries," *Energy*, vol. 210, Nov. 2020, Art. no. 118568. [Online]. Available: http://www.sciencedirect.com/science/article/pii/S0360544220316765

[14] A. C. Duman, H. S. Erden, Ö. Gönül, and Ö. Güler, "A home energy management system with an integrated smart thermostat for demand response in smart grids," *Sustain. Cities Soc.*, vol. 65, Feb. 2021, Art. no. 102639. [Online]. Available: https://www.sciencedirect.com/science/article/pii/S2210670720308556

[15] J. Wang, B. Chen, P. Li, and Y. Che, "Distributionally robust optimization of home energy management system based on receding horizon optimization," *Frontiers Energy*, vol. 14, no. 2, pp. 254–266, Jun. 2020, doi: 10.1007/s11708-020-0665-4.

[16] A. Akbari-Dibavar, S. Nojavan, B. Mohammadi-Ivatloo, and K. Zare, "Smart home energy management using hybrid robust-stochastic optimization," *Comput. Ind. Eng.*, vol. 143, May 2020, Art. no. 106425. [Online]. Available: http://www.sciencedirect.com/science/article/pii/S0360835220301595

[17] H. Mehrjerdi and E. Rakhshani, "Correlation of multiple time-scale and uncertainty modelling for renewable energy-load profiles in wind powered system," *J. Cleaner Prod.*, vol. 236, Nov. 2019, Art. no. 117644. [Online]. Available: https://www.sciencedirect.com/science/article/pii/S0959652619324941

[18] M. Talha, M. S. Saeed, G. Mohiuddin, M. Ahmad, M. J. Nazar, and N. Javaid, "Energy optimization in home energy management system using artificial fish swarm algorithm and genetic algorithm," in *Advances in Intelligent Networking and Collaborative Systems*, L. Barolli, I. Woungang, and O. K. Hussain, Eds. Cham, Switzerland: Springer, 2018, pp. 203–213.

[19] H. R. O. Rocha, I. H. Honorato, R. Fiorotti, W. C. Celeste, L. J. Silvestre, and J. A. L. Silva, "An artificial intelligence based scheduling algorithm for demand-side energy management in smart homes," *Appl. Energy*, vol. 282, Jan. 2021, Art. no. 116145. [Online]. Available: https://www.sciencedirect.com/science/article/pii/S0306261920315555

[20] J. Leitão, P. Gil, B. Ribeiro, and A. Cardoso, "Improving household's efficiency via scheduling of water and energy appliances," in *Proc. 13th APCA Int. Conf. Control Soft Comput. (CONTROLO)*, Jun. 2018, pp. 253–258.

[21] K. Ma, S. Hu, J. Yang, X. Xu, and X. Guan, "Appliances scheduling via cooperative multi-swarm PSO under day-ahead prices and photovoltaic generation," *Appl. Soft Comput.*, vol. 62, pp. 504–513, Jan. 2018.

[22] M. M. U. Rashid, F. Granelli, M. A. Hossain, M. S. Alam, F. S. Al-Ismail, A. K. Karmaker, and M. M. Rahaman, "Development of home energy management scheme for a smart grid community," *Energies*, vol. 13, no. 17, p. 4288, Aug. 2020. [Online]. Available:https://www.mdpi.com/1996-1073/13/17/4288

[23] J. Leitão, P. Gil, B. Ribeiro, and A. Cardoso, "Application of bees algorithm to reduce household's energy costs via load deferment," in *Proc. 10th Int. Conf. Inf. Technol. Electr. Eng. (ICITEE)*, Jul. 2018, pp. 100–105.

[24] M. M. Iqbal, M. I. A. Sajjad, S. Amin, S. S. Haroon, R. Liaqat, M. F. N. Khan, M. Waseem, and M. A. Shah, "Optimal scheduling of residential home appliances by considering energy storage and stochastically modelled photovoltaics in a grid exchange environment using hybrid grey wolf genetic algorithm optimizer," *Appl. Sci.*, vol. 9, no. 23, p. 5226, Dec. 2019. [Online]. Available: https://www.mdpi.com/2076-3417/9/23/5226

[25] I. O. Essiet, Y. Sun, and Z. Wang, "Optimized energy consumption model for smart home using improved differential evolution algorithm," *Energy*, vol. 172, pp. 354–365, Apr. 2019. [Online]. Available: http://www.sciencedirect.com/science/article/pii/S0360544219301537

[26] T. Pamulapati, R. Mallipeddi, and M. Lee, "Multi-objective home appliance scheduling with implicit and interactive user satisfaction modelling," *Appl. Energy*, vol. 267, Jun. 2020, Art. no. 114690. [Online]. Available: http://www.sciencedirect.com/science/article/pii/S0306261920302026

[27] R. Godina, E. M. G. Rodrigues, E. Pouresmaeil, and J. P. S. Catalão, "Optimal residential model predictive control energy management performance with PV microgeneration," *Comput. Oper. Res.*, vol. 96, pp. 143–156, Aug. 2018. [Online]. Available: http://www.sciencedirect.com/science/article/pii/S0305054817302952

[28] R. Godina, E. Rodrigues, E. Pouresmaeil, J. Matias, and J. Catalão, "Model predictive control home energy management and optimization strategy with demand response," *Appl. Sci.*, vol. 8, no. 3, p. 408, Mar. 2018. [Online]. Available:https://www.mdpi.com/2076-3417/8/3/408

[29] G. Bianchini, M. Casini, D. Pepe, A. Vicino, and G. G. Zanvettor, "An integrated model predictive control approach for optimal HVAC and energy storage operation in large-scale buildings," *Appl. Energy*, vol. 240, pp. 327–340, Apr. 2019. [Online]. Available: http://www.sciencedirect.com/science/article/pii/S030626191930162X

[30] M. R. Zavvar Sabegh and C. Bingham, "Model predictive control with binary quadratic programming for the scheduled operation of domestic refrigerators," *Energies*, vol. 12, no. 24, p. 4649, Dec. 2019. [Online]. Available: https://www.mdpi.com/1996-1073/12/24/4649

[31] H. Nagpal, A. Staino, and B. Basu, "Application of predictive control in scheduling of domestic appliances," *Appl. Sci.*, vol. 10, no. 5, p. 1627, Feb. 2020. [Online]. Available:https://www.mdpi.com/2076-3417/10/5/1627/htm

[32] B. Li and R. Roche, "Optimal scheduling of multiple multi-energy supply microgrids considering future prediction impacts based on model predictive control," *Energy*, vol. 197, Apr. 2020, Art. no. 117180. [Online]. Available: http://www.sciencedirect.com/science/article/pii/S0360544220302875

[33] I. Antonopoulos, V. Robu, B. Couraud, D. Kirli, S. Norbu, A. Kiprakis, D. Flynn, S. Elizondo-Gonzalez, and S. Wattam, "Artificial intelligence and machine learning approaches to energy demand-side response: A systematic review," *Renew. Sustain. Energy Rev.*, vol. 130, Sep. 2020, Art. no. 109899. [Online]. Available: https://www.sciencedirect.com/science/article/pii/S136403212030191X

[34] C. Yang, Q. Cheng, P. Lai, J. Liu, and H. Guo, *Data-Driven Modeling for Energy Consumption Estimation*. Cham, Switzerland: Springer, 2018, pp. 1057–1068, doi: 10.1007/978-3-319-62575-1_72.

[35] D. L. Y. Guan, S. Xue, and Y. Xi, "Feature-fusion-kernel-based Gaussian process model for probabilistic long-term load forecasting," *Neurocomputing*, vol. 426, pp. 174–184, Feb. 2021. [Online]. Available: http://www.sciencedirect.com/science/article/pii/S0925231220315964

[36] E. Spiliotis, H. Doukas, V. Assimakopoulos, and F. Petropoulos, "Forecasting week-ahead hourly electricity prices in Belgium with statistical and machine learning methods," in *Mathematical Modelling of Contemporary Electricity Markets*, A. Dagoumas, Ed. New York, NY, USA: Academic, 2021, pp. 59–74. [Online]. Available: https://www.sciencedirect.com/science/article/pii/B9780128218389000050

[37] O. I. Abiodun, A. Jantan, A. E. Omolara, K. V. Dada, N. A. Mohamed, and H. Arshad, "State-of-the-art in artificial neural network applications: A survey," *Heliyon*, vol. 4, no. 11, Nov. 2018, Art. no. e00938. [Online]. Available: https://www.sciencedirect.com/science/article/pii/S2405844018332067

[38] D. Zhang, X. Han, and C. Deng, "Review on the research and practice of deep learning and reinforcement learning in smart grids," *CSEE J. Power Energy Syst.*, vol. 4, no. 3, pp. 362–370, Sep. 2018.

[39] P. Kofinas, A. I. Dounis, and G. A. Vouros, "Fuzzy Q-learning for multi-agent decentralized energy management in microgrids," *Appl. Energy*, vol. 219, pp. 53–67, Jun. 2018. [Online]. Available: http://www.sciencedirect.com/science/article/pii/S0306261918303465

[40] F. Alfaverh, M. Denai, and Y. Sun, "Demand response strategy based on reinforcement learning and fuzzy reasoning for home energy management," *IEEE Access*, vol. 8, pp. 39310–39321, 2020.

[41] S. Lee and D.-H. Choi, "Energy management of smart home with home appliances, energy storage system and electric vehicle: A hierarchical deep reinforcement learning approach," *Sensors*, vol. 20, no. 7, p. 2157, Apr. 2020. [Online]. Available:https://www.mdpi.com/1424-8220/20/7/2157

[42] H.-M. Chung, S. Maharjan, Y. Zhang, and F. Eliassen, "Distributed deep reinforcement learning for intelligent load scheduling in residential smart grids," *IEEE Trans. Ind. Informat.*, vol. 17, no. 4, pp. 2752–2763, Apr. 2021.

[43] M. Latifi, A. Rastegarnia, A. Khalili, V. Vahidpour, and S. Sanei, "A distributed game-theoretic demand response with multi-class appliance control in smart grid," *Electr. Power Syst. Res.*, vol. 176, Nov. 2019, Art. no. 105946. [Online]. Available: http://www.sciencedirect.com/science/article/pii/S0378779619302652

[44] P. Kehoe and T. Chang, "Onsite water reuse: A collaborative strategy to manage water," in *Sustainable Industrial Water Use, Perspectives, Incentives, and Tools*. London, U.K.: IWA Publishing, Feb. 2021, doi: 10.2166/9781789060676_0271.

[45] B. Lokeshgupta and S. Sivasubramani, "Multi-objective home energy management with battery energy storage systems," *Sustain. Cities Soc.*, vol. 47, May 2019, Art. no. 101458. [Online]. Available: http://www.sciencedirect.com/science/article/pii/S2210670718312496

[46] F. Ouimet, "On the Le cam distance between Poisson and Gaussian experiments and the asymptotic properties of Szasz estimators," *J. Math. Anal. Appl.*, vol. 499, no. 1, Jul. 2021, Art. no. 125033. [Online]. Available: https://www.sciencedirect.com/science/article/pii/S0022247X21001128

[47] J. Widen, "Correlations between large-scale solar and wind power in a future scenario for Sweden," *IEEE Trans. Sustain. Energy*, vol. 2, no. 2, pp. 177–184, Apr. 2011.

[48] W. Holmgren, C. Hansen, and M. Mikofski, "Pvlib Python: A PyThon package for modeling solar energy systems," *J. Open Source Softw.*, vol. 3, no. 29, p. 884, 2018.
[49] M. Iqbal, *An Introduction to Solar Radiation*. New York, NY, USA: Academic, 1983.
[50] D. P. Larson, L. Nonnenmacher, and C. F. M. Coimbra, "Day-ahead forecasting of solar power output from photovoltaic plants in the American Southwest," *Renew. Energy*, vol. 91, pp. 11–20, Jun. 2016.
[51] M. Javan Salehi and M. Shourian, "Comparative application of model predictive control and particle swarm optimization in optimum operation of a large-scale water transfer system," *Water Resour. Manage.*, vol. 35, no. 2, pp. 707–727, Jan. 2021.
[52] Y. Chen, J. Ma, P. Zhang, F. Liu, and S. Mei, "Robust state estimator based on maximum exponential absolute value," *IEEE Trans. Smart Grid*, vol. 8, no. 4, pp. 1537–1544, Jul. 2017.
[53] Y. Chen, Y. Yao, and Y. Zhang, "A robust state estimation method based on SOCP for integrated electricity-heat system," *IEEE Trans. Smart Grid*, vol. 12, no. 1, pp. 810–820, Jan. 2021.
[54] Z. Fang, Y. Lin, S. Song, C. Li, X. Lin, and Y. Chen, "State estimation for situational awareness of active distribution system with photovoltaic power plants," *IEEE Trans. Smart Grid*, vol. 12, no. 1, pp. 239–250, Jan. 2021.
[55] A. Gleixner, L. Eifler, T. Gally, G. Gamrath, P. Gemander, R. L. Gottwald, G. Hendel, C. Hojny, T. Koch, M. Miltenberger, and B. Müller, "The SCIP optimization suite 6.0," Optim. Online, Tech. Rep., Jul. 2018. [Online]. Available: http://www.optimization-online.org/DB_HTML/2018/07/6692.html
[56] A. Gleixner, L. Eifler, T. Gally, G. Gamrath, P. Gemander, R. L. Gottwald, G. Hendel, C. Hojny, T. Koch, M. Miltenberger, and B. Müller, "The SCIP optimization suite 6.0," Zuse Inst. Berlin, Berlin, Germany, Tech. Rep. ZIB 18-26, Jul. 2018. [Online]. Available: http://nbn-resolving.de/urn:nbn:de:0297-zib-69361

JOAQUIM LEITÃO received the Licenciate and M.Sc. degrees in informatics engineering from the University of Coimbra, where he is currently pursuing the Ph.D. degree. He is also a Researcher with the Adaptive Computation (AC) Group, Center of Informatics and Systems of the University of Coimbra (CISUC). His research interests include cyber-physical systems, optimized energy management, smart homes and smart grid, human-in-the-loop systems, wired and wireless sensor, and actuator networks.

CARLOS M. FONSECA received the Electronic and Telecommunications Engineering degree from the University of Aveiro, Portugal, in 1991, and the Ph.D. degree from The University of Sheffield, U.K., in 1996. He is currently an Associate Professor with the Department of Informatics Engineering, University of Coimbra, Portugal, and a member of the Adaptive Computation (AC) Group, Centre for Informatics and Systems of the University of Coimbra (CISUC). Formerly, he was a Research Associate with the Department of Automatic Control and Systems Engineering, The University of Sheffield, and a Lecturer with the Department of Electronic Engineering and Informatics, Faculty of Science and Technology, University of Algarve, Portugal. His current research interests include multiobjective optimization, evolutionary algorithms, experimental assessment of algorithms, dynamical systems, and engineering design optimization.

PAULO GIL was born in Lisbon, Portugal. He received the Licentiate degree in mechanical engineering and the M.Sc. degree in informatics engineering with a focus on system and information technologies from the University of Coimbra, Coimbra, Portugal, and the Ph.D. degree in electrical engineering from the Universidade NOVA de Lisboa, Lisbon, with a focus on automatic control. He is currently an Assistant Professor with the Department of Electrical and Computer Engineering, NOVA School of Science and Technology and Research, Center of Informatics and Systems of the University of Coimbra (CISUC), and the Centre of Technology and Systems (CTS-UNINOVA). His current research interests include intelligent control, resilient networked control, hybrid control, multi-agent systems, and cyber-physical systems.

BERNARDETE RIBEIRO (Senior Member, IEEE) received the Ph.D. and Habilitation degrees in informatics engineering from the University of Coimbra, Portugal. She was the former President of the Portuguese Association of Pattern Recognition. She is currently a Full Professor with the Department of Informatics Engineering, University of Coimbra. She is also the Director of the Center of Informatics and Systems of University of Coimbra (CISUC), and the Founder and the Director of the Laboratory of Artificial Neural Networks for over 20 years. Her research interests include machine learning, and pattern recognition, and their applications to a broad range of fields. She has been responsible/participated in several research projects both at international and national levels in a wide range of application areas. She is an IEEE SMC Senior Member, and a member of the IARP International Association of Pattern Recognition, the International Neural Network Society, and the Association for Computing Machinery. She is also an Associate Editor of IEEE TRANSACTIONS ON CYBERNETICS.

ALBERTO CARDOSO was born in Coimbra, Portugal. He received the Licentiate degree in electrical engineering, the M.Sc. degree in systems and information technologies with a focus on systems and control, and the Ph.D. degree in informatics engineering from the University of Coimbra. He is currently an Assistant Professor with the Department of Informatics Engineering (DEI), University of Coimbra, and a Senior Researcher with the Centre for Informatics and Systems of the University of Coimbra (CISUC), where he is responsible for the Laboratory of Industrial Informatics and Systems. He coordinates/participates in national and international projects, such as H2020 KYKLOS4.0, H2020 ReMAP, SUDOE NanoSen-AQM, and FCT FireLoc. His main research interests include cyber-physical systems, data analytics, intelligent systems, sensor data fusion, remote and virtual laboratories, geographic information systems, and fault tolerant control. He was awarded the title "International Engineering Educator Honoris Causa" by the International Society for Engineering Pedagogy (IGIP). He was the President of the Portuguese Association of Automatic Control (APCA) and the Portuguese Society for Engineering Education (SPEE), and the Coordinator of the Informatics Engineering Chapter for the Centre Region of the Portuguese Engineering Association.